NASA Contractor Report 189690
ICASE Report No. 92–37

ICASE

SINGULARITIES IN THE CLASSICAL RAYLEIGH-TAYLOR FLOW: FORMATION AND SUBSEQUENT MOTION

S. Tanveer

Contract No. NAS1–18605
August 1992

Institute for Computer Applications in Science and Engineering
NASA Langley Research Center
Hampton, Virginia 23665–5225

Operated by the Universities Space Research Association

National Aeronautics and
Space Administration

Langley Research Center
Hampton, Virginia 23665-5225

SINGULARITIES IN THE CLASSICAL RAYLEIGH-TAYLOR FLOW: FORMATION AND SUBSEQUENT MOTION

S. Tanveer*
Mathematics Department
Ohio State University
Columbus, OH 43210

ABSTRACT

This paper is concerned with the creation and subsequent motion of singularities of solution to classical Rayleigh-Taylor flow (two dimensional inviscid, incompressible fluid over a vacuum). For a specific set of initial conditions, we give analytical evidence to suggest the instantaneous formation of one or more singularity(ies) at specific point(s) in the unphysical plane, whose locations depend sensitively to small changes in initial conditions in the physical domain. One-half power singularities are created in accordance with an earlier conjecture; however, depending on initial conditions, other forms of singularities are also possible.

For a specific initial condition, we follow a numerical procedure in the unphysical plane to compute the motion of a one-half singularity. This computation confirms our previous conjecture that the approach of a one-half singularity towards the physical domain corresponds to the development of a spike at the physical interface. Under some assumptions that appear to be consistent with numerical calculations, we present analytical evidence to suggest that a singularity of the one-half type cannot impinge the physical domain in finite time.

*Research was supported by the National Aeronautics and Space Administration under NASA Contract No. NAS1-18605 while the author was in residence at the Institute for Computer Applications in Science and Engineering (ICASE), NASA Langley Research Center, Hampton, VA 23665.

1. INTRODUCTION

The motion of the interface of a heavy fluid initially resting on top of a lighter fluid (Rayleigh-Taylor flow) is a very basic but important problem in fluid dynamics and has been the subject of intensive research over a long period of time. Recent interest in the Rayleigh-Taylor instability stems from its disruptive presence in inertial confinement devices (See Verdon et al (1982) for instance). Emmons, Chang & Watson (1959) studied the interfacial features experimentally with initially sinusoidal disturbances and found that for large times, a pattern containing downward spikes and upward moving bubbles forms. In other experiments (Read, 1984) with Atwood ratio close to one (i.e. density ratio between lighter and heavier fluid close to zero), a variety of bubbles and spikes is formed for random initial condition. It is clear that there is a significant interaction between bubbles (or spikes) so that the congregate motion is rather different from a regular pattern.

In the idealized limit of two-dimensional inviscid, incompressible fluid over a vacuum, direct numerical calculations by Baker, Meiron & Orszag (1982) have shown that an initial sinusoidal perturbation of the interface leads to an upward moving bubble and a downward moving spike in each period of the disturbance. The shape of the upward moving bubble agrees with the steady bubble solutions of Davies & Taylor (1950), while a downward moving spike accelerates with free fall. For initial conditions containing more than one non-identical undulation per period, the demand for appropriate resolution makes it difficult to continue calculations (along the lines of Baker, Meiron & Orszag (1982)) for sufficiently long-times to identify the effective acceleration of the bubble-tip-envelope observed in the Read experiment (1984).

Given the physical importance of its dynamics, the Rayleigh-Taylor problem has also been studied from a more practical perspective since direct numerical calculations based on the fluid-dynamical equations appear to be impractical even for the simplest of the Rayleigh-Taylor flows. Model equations have been developed (see Gardner et al (1988) and Sharp (1984) and references there in) to study the interaction of multiple bubbles and spikes. Typically these include parameters that in some cases can be computed rationally by appeal to physical dynamics. Some of the more recent models (Gardner et al (1988)) have been developed in great generality without any of the restrictive assumptions of an inviscid incompressible two dimensional flow. While these studies have been quite important in furthering physical understanding of bubble competition and merger processes, we are unaware of any direct derivation of model equations from the fundamental fluid equations. While this paper does not address this problem either, we hope the approach in this paper will eventually bridge the gap between the direct numerical simulation of fluid equations and model studies, at least in simple cases.

Here, we explore the dynamics of singularities in the classical Rayleigh-Taylor problem without resort to any localized approximation (Siegel (1989), Baker, Caflisch & Siegel (1992)). At time t, consider the conformal map $z(\zeta, t)$ that maps the interior of a cut unit circle in the ζ plane (Fig. 1) into a periodic strip in the physical domain (Fig. 2) such that the origin coincides with $z = -i\,\infty$. The unit circular boundary then corresponds to the free boundary. We will be concerned with the formation and subsequent motion of singularities of $z(\zeta, t)$ and the complex velocity potential $W(\zeta, t)$ in the unphysical domain $|\zeta| > 1$. We have several long range goals in furthering such an understanding.

First is the possibility that singularities can be analytically subtracted out in a basis representation of f and W making them amenable to direct numerical calculations for a long time. Second is that the bubble and spike interaction can be understood through the interaction of multiple singularities in the unphysical complex plane. As shown in this paper, a one-half singularity in $|\zeta| > 1$ approaching $|\zeta| = 1$ corresponds to a continually developing spike at the physical interface. The portion of the unit circle $|\zeta| = 1$ between any two approaching singularities contains the image of the bubble boundary in the ζ plane. Thus, pairwise singularity merging corresponds to a bubble getting smaller, while its neighbor becomes larger–a well known process in the Rayleigh-Taylor problem. Third, it may be possible to reach general qualitative and quantitative conclusions about the relation of long time bubble dynamics to the specifics of initial conditions in the complex unphysical plane, which is related to the physical initial condition in an ill-posed way. This may allow one to construct an appropriate statistical model of bubble interaction in terms of the statistical features of the initial conditions in the unphysical domain.

In a previous paper (Tanveer, 1991a), the analytically continued equations for the two-dimensional Rayleigh-Taylor and water wave problems were derived in the unphysical domain $|\zeta| > 1$. For steady water waves, analytical and numerical calculations were carried out to establish the relation of water wave crests to one-half singularities of $z(\zeta, t)$. However, for the Rayleigh-Taylor or the unsteady water wave problems, no concrete results were obtained except to note that certain one-half singularities of $z(\zeta, t)$ and $W(\zeta, t)$ were consistent with these equations. It was also noted that in the limit of a one-half singularity approaching the physical domain, the analytically continued acceleration at a one-half singularity is the free-fall under gravity, similar to that which is observed for a spike. Based on this, it was conjectured that a one-half singularity approaching the physical domain corresponds to a spike developing at the physical interface. The work presented here is is a natural continuation of our previous (Tanveer, 1991a) work. This paper is organized as follows.

In Section 2, we present the analytically continued equations in the unphysical plane

$|\zeta| > 1$ that has been derived previously (Tanveer, 1991a). The equations are presented in several alternate forms, some more convenient for asymptotic analysis, while others for numerical computation.

In Section 3, we show that under some assumptions on the single-valuedness of ζ as a function of a characteristic variable in some region of the characteristic space, the only possible singularity $\zeta_s(t)$ of $z(\zeta,t)$ and $W(\zeta,t)$ in ζ is of a "fold" type where each of $\frac{1}{z_\zeta}$ and $\frac{W_\zeta}{z_\zeta}$ are analytic functions of the variable $(\zeta-\zeta_s(t))^{1/2}$ or $(\zeta-\zeta_s(t))^{1/3}$ or $(\zeta-\zeta_s(t))^{1/4}$, etc. In the case when the fold singularity is of the one-half type, we relate the coefficients in an expansion in $[\zeta-\zeta_s(t)]^{1/2}$ to the solution in the characteristic plane.

In Section 4, we address the question of singularity formation–how does a singularity of $z(\zeta,t)$ and $W(\zeta,t)$ form in the unphysical domain when there is none initially? We consider several classes of initial conditions for which $z(\zeta,0)$ and $W(\zeta,0)$ are analytic everywhere in the finite ζ plane outside the unit circle. We give analytical evidence to suggest that singularities can form instantaneously at a point in the ζ plane where $z_\zeta(\zeta,0)=0$. This result is very similar to results obtained in similar situations for other fluid flows such as the Hele-Shaw flow with surface tension (Tanveer (1991b)) or the Kelvin-Helmholtz problem. In the latter case, recent work of Cowley et al (1992) has shown that the Moore singularity (Moore (1979,1985), supported by numerical computations of Krasny (1986), Shelly (1992) and rigorously analyzed by Caflisch & Orlenna (1988), actually forms instantaneously at some point in the complex circulation variable. We also find that in our problem, for some initial conditions, a singularity moves in instantaneously from infinity to the finite ζ plane in the sense that for any fixed $t > 0$, the singularity is at a finite ζ point; yet as $t \to 0^+$, this location recedes to infinity. Our calculations suggests that for certain set of initial conditions, only one-half singularities can be created; however, there exists other initial conditions for which singularities of a more complicated form involving logarithm can occur. In this case, the assumption on single valuedness of $\zeta(\xi,t)$ that is assumed in the analysis of Section 3 is violated.

In Section 5, we employ a numerical procedure to track the motion of a one-half singularity that is created at the initial instant of time. We compute not only the location, but also a few coefficients of the one-half power expansion. So far, numerical computation has been performed for a very special initial condition. Nonetheless, the result confirms our previous conjecture that the approach of a one-half singularity corresponds to a continually developing spike at the physical interface.

In Section 6, we address the question if an approaching one-half singularity of $z(\zeta,t)$ and $W(\zeta,t)$ of the type computed in Section 5 can actually impinge the physical domain boundary $|\zeta|=1$ in finite time. With certain assumptions that appear to be consistent

with the numerical calculations in Section 5, our analytical evidence suggests that an isolated one-half singularity cannot impinge the real domain in finite time. However, this leaves open the possibility of different kinds of singularity or multiple one-half singularities coalescing at $|\zeta| = 1$. This result has a bearing on the work of other researchers. Siegel (1989) and Baker, Caflisch & Siegel (1992) have studied exact complex travelling wave solutions to a localized simplification of the Rayleigh-Taylor equations for arbitrary Atwood ratio. For unit Atwood ratio (the case studied here), Baker, Caflisch & Orlenna (1992) found a class of travelling wave solutions with one-half singularities, each of which moves at a constant speed. However, based on a spectrum fit of the numerically computed results for the full Rayleigh-Taylor problem in the physical domain, they detect a definite slow down of such singularities at unit Atwood ratio which is at variance with the solution to the localized approximation. However, it remains unclear from their work if the slowdown was sufficiently significant to avoid a finite time singularity in the real domain.

Since the analytic continuation of $z(\zeta,0)$ from $|\zeta| \leq 1$ to the unphysical plane $|\zeta| > 1$ is an ill-posed procedure, i.e. arbitrary small deviations of $z(\zeta,0)$ in $|\zeta| \leq 1$ can affect the location of its zeros of $z_\zeta(\zeta,0)$ in $|\zeta| > 1$, it follows that the precise location and number of such singularities created at initial time will be highly sensitive to initial conditions in the physical domain. Our results on the correspondence of singularities with spikes at later times can explain the observed random nature of bubble-spike interaction in the long-term behavior of the physical interface. In our discussion in Section 7, we make a plausibility argument on how singularity interactions can explain bubble competition.

2. MATHEMATICAL EQUATIONS

The conformal map from the cut unit ζ circle (Fig. 1) into a periodic strip in the physical domain as shown in Fig. 2 ($z = x + iy$) can be decomposed into

$$z(\zeta,t) \;=\; 2\,\pi \;+\; i\;ln\;\zeta \;+\; i\;f(\zeta,t) \tag{2.1}$$

where $f(\zeta,t)$ is oblivious to the branch cut and therefore possesses a convergent power series representation for $|\zeta| < 1$

$$f(\zeta,t) \;=\; \sum_{n=0}^{\infty} a_n(t)\;\zeta^n\,. \tag{2.2}$$

Here we have assumed, without any loss of generality, that the period in the z plane is 2π and the acceleration due to gravity is unity and is directed upwards (along the positive y axis). For analytic shape, the convergence of (2) occurs up to $|\zeta| = 1$. Similarly, there exists a power series representation for the complex velocity potential

$$W(\zeta,t) \;=\; \sum_{n=0}^{\infty} b_n(t)\;\zeta^n\,. \tag{2.3}$$

We will assume that the initial conditions are symmetric, so that a_n and b_n are initially real. From the equations, it is clear that these symmetries are preserved for all later times. This assumption is only made for simplicity and generalizations for nonsymmetric disturbances are possible. This means that on the real ζ -axis in the interval (-1,1),

$$Im\ f\ =\ 0 \tag{2.4}$$

holds for f and the complex velocity potential W satisfies

$$Im\ W\ =\ 0\,. \tag{2.5}$$

The kinematic condition on the free boundary can be expressed as

$$\frac{D}{Dt}\ ln\ \rho(x,y,t)\ =\ 0 \tag{2.6}$$

on $\rho(x,y,t)\ =\ 1$, where $\zeta\ =\ \rho\ e^{i\nu}$, with ν real. In this representation, $ln\ \rho$, ν and t can be thought of as three dependent variables depending on x , y and t . Switching the role of dependent and independent variables, the kinematic condition implies that

$$Re\ \left[\ \zeta\ W_\zeta\ -\ \zeta^*\ z_\zeta^*\ z_t\right]\ =\ 0 \tag{2.7}$$

where the symbol $*$ here and in what follows stands for complex conjugation. Plugging in the representation for z from (2.1) on $|\zeta|\ =\ 1$, we find that (2.7) is equivalent to

$$Re\ \left[\ \frac{f_t}{1\ +\ \zeta\ f_\zeta}\right]\ =\ \frac{Re\ \zeta W_\zeta}{|1\ +\ \zeta\ f_\zeta|^2} \tag{2.8}$$

on $\zeta\ =\ e^{i\nu}$ for ν in the interval $[0,\ 2\ \pi]$. The analytic continuation of this for $|\zeta|\ >\ 1$ (see Tanveer, 1991a for details) is

$$\frac{f_t}{1\ +\ \zeta\ f_\zeta}\ -\ \frac{\zeta\ W_\zeta\ +\ \frac{1}{\zeta}\ W_\zeta(1/\zeta,t)}{(1+\zeta\ f_\zeta)\ (1+\frac{1}{\zeta}f_\zeta(1/\zeta,t))}\ =\ I_2 \tag{2.9}$$

where I_2 can be written as either of the following two expressions

$$I_2(\zeta,t)\ =\ -\ \frac{f_t(1/\zeta,t)}{1+\frac{1}{\zeta}f_\zeta(\frac{1}{\zeta},t)} \tag{2.10}$$

$$I_2(\zeta,t)\ =\ \frac{1}{4\pi i}\ \oint_{|\zeta'|=1}\ \frac{d\zeta'}{\zeta'}\ \left[\frac{\zeta+\zeta'}{\zeta'-\zeta}\right]\ \frac{\zeta' W_\zeta(\zeta',t)\ +\ \frac{1}{\zeta'}\ W_\zeta(\frac{1}{\zeta'},t)}{[1+\zeta'\ f_\zeta(\zeta',t)]\ [1+\frac{1}{\zeta'}\ f_\zeta(\frac{1}{\zeta'},t)]}\,. \tag{2.11}$$

The Bernoulli's condition on the free surface for this time dependent problem can be written as

$$Re\ [\ W_t\ -\ \frac{\zeta W_\zeta f_t}{1+\zeta f_\zeta}\ -\ f]\ =\ -\ \frac{1}{2}\ \frac{|W_\zeta|^2}{|1+\zeta f_\zeta|^2} \tag{2.12}$$

on the unit circle $\zeta\ =\ e^{i\ \nu}$. The analytic continuation of this outside the unit circle (see Tanveer, 1991a for details) is

$$W_t\ -\ \frac{\zeta\ W_\zeta\ f_t}{1\ +\ \zeta\ f_\zeta}\ -\ f\ +\ \frac{W_\zeta\ W_\zeta(1/\zeta,t)}{(1+\zeta\ f_\zeta)\ (1+\frac{1}{\zeta}+f_\zeta(1/\zeta,t))}\ =\ -I_1 \tag{2.13}$$

where I_1 can be written in either of the following two representations

$$I_1(\zeta,t)\ =\ W_t(1/\zeta,t)-\frac{\frac{1}{\zeta}W_\zeta(\frac{1}{\zeta},t)f_t(\frac{1}{\zeta},t)}{(1\ +\ \frac{1}{\zeta}f_\zeta(\frac{1}{\zeta},t))}\ -\ f(\frac{1}{\zeta},t) \tag{2.14}$$

$$I_1(\zeta,t)\ =\ \frac{1}{4\pi i}\ \oint_{|\zeta'|=1}\frac{d\zeta'}{\zeta'}\ \left[\frac{\zeta+\zeta'}{\zeta'-\zeta}\right]\ \frac{W_\zeta(\zeta',t)\ W_\zeta(\frac{1}{\zeta'},t)}{[1+\zeta'\ f_\zeta(\zeta',t)]\ [1+\frac{1}{\zeta'}\ f_\zeta(\frac{1}{\zeta'},t)]}\,. \tag{2.15}$$

Equations (2.7) and (2.13) can be written in a more convenient form by defining

$$y_1\ =\ \frac{\zeta W_\zeta}{1+\zeta f_\zeta} \tag{2.16}$$

$$y_2\ =\ \frac{1}{1+\zeta f_\zeta}\,. \tag{2.17}$$

In that case, we get (Tanveer (1991a))

$$y_{1_t}-(R_3+R_2y_1)y_{1_\zeta}\ =\ \zeta y_1y_2R_{1_\zeta}\ -\ (1+\zeta I_{1_\zeta})y_2+1 \tag{2.18}$$

$$y_{2_t}-(R_3+R_2y_1)y_{2_\zeta}=-R_2y_2y_{1_\zeta}+\frac{R_3}{\zeta}y_2-\frac{R_3}{\zeta}y_2^2-\zeta R_{4_\zeta}y_2^2-\zeta(\frac{R_2}{\zeta})_\zeta y_1y_2-R_{3_\zeta}y_2+R_{3_\zeta}y_2^2 \tag{2.19}$$

where

$$R_1\ =\ -\ \frac{\frac{1}{\zeta}\ W_\zeta(\frac{1}{\zeta},t)}{1\ +\ \frac{1}{\zeta}\ f_\zeta(\frac{1}{\zeta},t)}\ =\ -y_1(\frac{1}{\zeta},\ t) \tag{2.20}$$

$$R_2\ =\ \frac{\zeta}{1\ +\ \frac{1}{\zeta}\ f_\zeta(\frac{1}{\zeta},t)}\ =\ \zeta\ y_2(\frac{1}{\zeta},t) \tag{2.21}$$

$$R_3\ =\ \zeta\ I_2 \tag{2.22}$$

$$R_4\ =\ I_2\ +\ \frac{\frac{1}{\zeta}\ W_\zeta(\frac{1}{\zeta},t)}{1\ +\ \frac{1}{\zeta}\ f_\zeta(\frac{1}{\zeta},t)}\ =\ I_2\ +\ y_1(\frac{1}{\zeta},t)\,. \tag{2.23}$$

Notice that $I_1(\zeta,t)$ and $I_2(\zeta,t)$ given by (2.15) and (2.10) can also be written as

$$I_1(\zeta,t) \;=\; \frac{1}{4\pi i}\oint_{|\zeta'|=1}\frac{d\zeta'}{\zeta'}\left[\frac{\zeta+\zeta'}{\zeta'-\zeta}\right]\;|y_1(\zeta',t)|^2 \tag{2.24}$$

$$I_2(\zeta,t) \;=\; \frac{1}{2\pi i}\oint_{|\zeta'|=1}\frac{d\zeta'}{\zeta'}\left[\frac{\zeta+\zeta'}{\zeta'-\zeta}\right]\;Re\;[y_1^*(\zeta',t)y_2(\zeta',t)] \tag{2.25}$$

since from symmetry properties (2.4) and (2.5) and the relations (2.16) and (2.17), $y_1^*(\zeta',t) = y_1(1/\zeta',t)$ and $y_2^*(\zeta',t) = y_2(1/\zeta',t)$ on $|\zeta'| = 1$. By using (2.18) and (2.19), equation (2.19) can be replaced by a relatively more compact equation

$$\left[\frac{1}{\zeta y_2}\right]_t - \left[(R_3 + R_2 y_1)\frac{1}{\zeta y_2}\right]_\zeta \;=\; -R_{1\zeta}\,. \tag{2.26}$$

By introducing an appropriate characteristic variable ξ such that $\zeta = \zeta(\xi,t)$ and $\zeta(\xi,0) = \xi$ and defining

$$\hat{y}_1(\xi,t) = y_1(\zeta(\xi,t),t) \tag{2.27}$$

$$\hat{y}_2(\xi,t) = \frac{y_2(\zeta(\xi,t),t)}{\zeta_\xi(\xi,t)}\,, \tag{2.28}$$

one finds that equations (2.18) and (2.19) is equivalent to the following set of equations for $\zeta(\xi,t)$, $\hat{y}_1(\xi,t)$ and $\hat{y}_2(\xi,t)$ (Tanveer (1991a))

$$\zeta_t = -R_3 - R_2\hat{y}_1 \tag{2.29}$$

$$\hat{y}_{1_t} \;=\; \zeta\hat{y}_1\hat{y}_2\;\zeta_\xi\;R_{1_\zeta} \;-\; (1+\zeta I_{1_\zeta})\hat{y}_2\;\zeta_\xi + 1 \tag{2.30}$$

$$\hat{y}_{2_t} \;=\; \frac{R_3}{\zeta}\hat{y}_2 \;-\; \frac{R_3}{\zeta}\;\hat{y}_2^2\;\zeta_\xi \;-\; \zeta\;R_{4\zeta}\;\zeta_\xi\;\hat{y}_2^2 \;+\; R_{3_\zeta}\;\zeta_\xi\;\hat{y}_2^2 \;+\; \frac{R_2}{\zeta}\hat{y}_1\hat{y}_2\,. \tag{2.31}$$

Alternatively, from (2.29)-(2.31), we can derive

$$\left[\frac{1}{\zeta\hat{y}_2}\right]_t \;=\; -R_{1\zeta}(\zeta(\xi,t),t)\zeta_\xi \tag{2.32}$$

$$\left[\frac{\hat{y}_1}{\zeta\hat{y}_2}\right]_t \;=\; -\;[1\;+\;\zeta\;I_{1\zeta}(\zeta(\xi,t),t)]\;\frac{\zeta_\xi}{\zeta}\;+\;\frac{1}{\zeta\hat{y}_2}\,. \tag{2.33}$$

Equations (2.29), (2.32) and (2.33) will form the basis of the numerical calculation described in Section 4.

3. PROPERTIES OF A CLASS OF SOLUTIONS

Consider initial conditions for which each of $z_\zeta(\zeta,0)$ and $W_\zeta(\zeta,0)$ are analytic everywhere in $|\zeta| > 1$ except possibly at ∞. Also, assume that there is some open region $\mathcal{R}$ in the ξ plane in $|\xi| > 1$ so that the image of R under $\zeta(\xi,t)$ up to certain time T is contained in $|\zeta| > 1$ with no point mapping to $\zeta = \infty$. Further, we require that $\zeta(\xi,t)$ is single valued in $\mathcal{R}$. These set of assumptions will be referred to later as Assumption A. Our results in the next section suggests that Assumption A can only be valid for arbitrary $\mathcal{R}$ in $|\xi| > 1$ for some class of initial conditions.

Consider an arbitrary closed contour C within $\mathcal{R}$ where the Assumption A above is valid up to some time $T > 0$. We now derive some analyticity properties of the solution in this region up to time T.

It follows from (2.32) that

$$\frac{d}{dt}\left[\oint_C d\xi\, \frac{1}{\zeta\, \hat{y}_2}\right] = 0. \tag{3.1}$$

Integration of (2.33) implies that

$$\frac{d}{dt}\left[\oint_C d\xi\, \frac{\hat{y}_1}{\zeta\, \hat{y}_2}\right] = \oint_C d\xi\, \frac{1}{\zeta\, \hat{y}_2}. \tag{3.2}$$

Initially, $\zeta(\xi,0) = \xi$ and $\hat{y}_1$ and $\hat{y}_2$ coincide with y_1 and y_2. Thus since $z_\zeta(\zeta,0)$ and $W_\zeta(\zeta,0)$ are each analytic (Assumption A), from (2.16) and (2.17), it follows that each of $\frac{1}{\zeta y_2(\zeta,0)}$ and $\frac{y_1(\zeta,0)}{\zeta y_2(\zeta,0)}$ is an analytic function of ζ for $|\zeta| > 1$ (except possibly at ∞). Thus, $\frac{1}{\zeta(\xi,0)\hat{y}_2(\xi,0)}$ and $\frac{\hat{y}_1(\xi,0)}{\zeta(\xi,0)\hat{y}_2(\xi,0)}$ are analytic functions of ξ for $|\xi| > 1$ (except possibly at ∞). Thus, from Cauchy's theorem

$$\left[\oint_C d\xi\, \frac{1}{\zeta(\xi,0)\, \hat{y}_2(\xi,0)}\right] = 0 \tag{3.3}$$

$$\left[\oint_C d\xi\, \frac{\hat{y}_1(\xi,0)}{\zeta(\xi,0)\, \hat{y}_2(\xi,0)}\right] = 0. \tag{3.4}$$

From (3.1) and (3.2), it follows that

$$\left[\oint_C d\xi\, \frac{1}{\zeta(\xi,t)\, \hat{y}_2(\xi,t)}\right] = 0 \tag{3.5}$$

$$\left[\oint_C d\xi\, \frac{\hat{y}_1(\xi,t)}{\zeta(\xi,t)\, \hat{y}_2(\xi,t)}\right] = 0. \tag{3.6}$$

Then from Moerara's theorem, $\frac{1}{\zeta(\xi,t)\hat{y}_2(\xi,t)}$ and $\frac{\hat{y}_1(\xi,t)}{\zeta(\xi,t)\hat{y}_2(\xi,t)}$ will be analytic in ξ in $\mathcal{R}$. Then, $\hat{y}_1(\xi,t)$ and $\hat{y}_2$ can only have pole singularities of the same order. However, from (2.20), a

pole in $\hat{y}_1$ is compatible only with a logarithmic or worse singularity of $\zeta(\xi,t)$, which therefore violates Assumption A. Thus, under Assumption A, we find that each of $\hat{y}_1$ and $\hat{y}_2$ will be an analytic function of ξ in the region $\mathcal{R}$.

However, despite the analyticity of $\hat{y}_1$ and $\hat{y}_2$ as a function of ξ under Assumption A, each of y_1 and y_2 (and therefore f and W) can have singularities in the image of $\mathcal{R}$ in the ζ plane, as we shall now see. A singularity appears whenever there is failure of local inversion of the relation $\zeta = \zeta(\xi,t)$ into $\xi = \xi(\zeta,t)$. Such a singularity will be referred to as a fold singularity as will occur a point $\xi_0(t)$ where

$$\zeta_\xi(\xi_0(t),t) = 0\,. \tag{3.7}$$

For a fold of the simplest kind,

$$\zeta_{\xi\xi}(\xi_0(t),t) \;\neq\; 0\,. \tag{3.8}$$

It is clear that if we define $\zeta_s(t) = \zeta(\xi_0(t),t)$, then near $\xi = \xi_0(t)$,

$$\zeta = \zeta_s(t) \;+\; \frac{1}{2}\zeta_{\xi\xi}(\xi_0(t),t)[\xi - \xi_0(t)]^2 \;+\; \ldots \tag{3.9}$$

$$\zeta_\xi = \zeta_{\xi\xi}(\xi_0(t),t)[\xi - \xi_0(t)] \;+\; \ldots \tag{3.10}$$

$$\hat{y}_1(\xi,t) = \hat{A}_1(t) + \hat{A}_2(t)(\xi - \xi_0(t)) \;+\; \hat{A}_3(t)(\xi - \xi_0(t))^2 \;+\; O(\xi - \xi_0(t))^2 \tag{3.11}$$

$$\hat{y}_2(\xi,t) = \hat{B}_2(t) + \hat{B}_3(\xi - \xi_0(t)) \;+\; O(\xi - \xi_0(t))^2\,. \tag{3.12}$$

Then, it is clear from (2.27), (2.28), (3.9)-(3.12) that

$$y_1(\zeta,t) \;=\; A_1(t) \;+\; A_2(t)\,(\zeta - \zeta_s(t))^{1/2} \;+\; A_3(\zeta - \zeta_s) \;+\; o(\zeta - \zeta_s)^{3/2}.. \tag{3.13}$$

and

$$y_2(\zeta,t) \;=\; B_2(t)\,(\zeta - \zeta_s(t))^{1/2} \;+\; B_3(t)(\zeta - \zeta_s) \;+\; o((\zeta - \zeta_s)^{3/2}).. \tag{3.14}$$

where

$$A_1(t) = \tilde{A}_1(t) \tag{3.15}$$

$$A_2(t) = \sqrt{\frac{2}{\zeta_{\xi\xi}(\xi_0(t),t)}}\hat{A}_2(t) \tag{3.16}$$

$$B_2(t) = \sqrt{2\zeta_{\xi\xi}(\xi_0(t),t)}\hat{B}_2(t)\,. \tag{3.17}$$

Similar expressions can be found for the other coefficients. Going through the inversion process carefully, it is clear that the analyticity of $\hat{y}_1$ and $\hat{y}_2$ at $\xi = \xi_0(t)$ implies that each

of $y_1(\zeta,t)$ and $y_2(\zeta,t)$ is analytic in $[\zeta-\zeta_s(t)]^{1/2}$ at $\zeta=\zeta_s(t)$. From the definition of y_1 and y_2 in (2.16) and (2.17) and that of f in (2.1), it follows that under Assumption A and condition (3.8), each of $z(\zeta,t)$ and $W(\zeta,t)$ will be analytic in $[\zeta-\zeta_s(t)]^{1/2}$ at $\zeta=\zeta_s(t)$.

The speed of such a singularity $\dot{\zeta}_s$ can be found by noticing that due to (3.7), $\frac{d}{dt}\zeta(\xi_0(t),t)=\zeta_t(\xi_0(t),t)$ since $\zeta_\xi(\xi_0(t),t)=0$ for a fold singularity. Therefore from (2.29),

$$\dot{\zeta}_s \;=\; -R_3(\zeta_s(t),t) \;-R_2(\zeta_s(t),t)\; y_1(\zeta_s(t),t)\,. \tag{3.18}$$

Alternatively, on substituting (3.13) and (3.14) directly into (2.18) and (2.19), we find that the coefficients of the most singular terms as $\zeta \;\rightarrow\; \zeta_s(t)$ is given by

$$A_2\;\frac{d}{dt}\zeta_s \;+\; A_2\;R_{3_0} \;+\; R_{2_0}A_2\;A_1 \;=\; 0 \tag{3.19}$$

and

$$B_2\frac{d}{dt}\zeta_s \;+\; (R_{3_0} \;+\; R_{2_0}A_1)B_2 \;=\; 0 \tag{3.20}$$

where subscript 0 refers to the evaluation of those quantities at $\zeta \;=\; \zeta_s(t)$. Note that each of equations (3.19) and (3.20) are consistent with (3.18). Equating progressively less singular terms in $\zeta-\zeta_s(t)$ obtained by substituting (3.13) and (3.14) into (2.18), we get a set of relations, the first two of which is

$$\dot{A}_1 \;=\; 1 \;+\; \frac{1}{2}\;A_2^2\;R_{2_\zeta}(\zeta_s(t),t) \tag{3.21}$$

$$\begin{aligned}\dot{A}_2 \;=\; &\frac{1}{2}\;[R_{3_\zeta}(\zeta_s(t),t) \;+\; R_{2_\zeta}(\zeta_s(t),t)\;A_1 \;+\; R_2(\zeta_s(t),t)A_3]A_2\\ &+\; R_2(\zeta_s(t),t)A_2A_3 \;+\; \zeta_sA_1B_2R_{1_\zeta}(\zeta_s(t),t) \;-\; (1+\zeta_sI_{1_\zeta}(\zeta_s(t),t))\;B_2\,.\end{aligned} \tag{3.22}$$

Similarly on substituting (3.13) and (3.14) into (2.26) and equating different powers of $(\zeta-\zeta_s)^{1/2}$, we find that the leading order equation is just (3.20). At the next order, we find

$$\begin{aligned}\frac{d}{dt}\;\left[\frac{1}{\zeta_sB_2}\right] \;=\; \frac{1}{2}\Bigg[\frac{1}{\zeta_sB_2}\;&(R_{3_\zeta}(\zeta_s(t),t) \;+\; R_{2_\zeta}(\zeta_s(t),t)\;A_1 \;+\; R_2\;(\zeta_s(t),t)\;A_3\;)\\ &-\; R_2(\zeta_s(t),t)A_2\frac{B_3}{B_2^2\zeta_s}\;\Bigg]\,.\end{aligned} \tag{3.23}$$

It is clear from this expansion that once A_1, A_2, $\zeta_s(t)$ $B_2(t)$ and $B_3(t)$ are known as a function of time, one can calculate the coefficients of the higher order terms (say A_3 and B_3) in terms of the already known lower order terms, provided global terms such as $R_3(\zeta_s(t),t)$ and $I_{1\,\zeta}(\zeta_s(t),t)$ are known. This is an important observation as it gives us, at

least in principle, a method of calculating as many coefficients in the one-half expansion in (3.13) and (3.14) as we want, provided the first few terms are known. In Section 5, we numerically calculate the first few coefficients and also show how the global terms can be calculated.

Using a similar procedure as above, it is clear that if $\xi_0(t)$ is a double zero of ζ_ξ and Assumption A holds, the expansion for $y_1(\zeta,t)$ and $y_2(\zeta,t)$ will contain powers of $(\zeta-\zeta_s(t))^{1/3}$. Generally for a zero of ζ_ξ of n-th degree, one can expect a series in $[\zeta-\zeta_s(t)]^{1/(n+1)}$ for each of y_1 and y_2.

4. SINGULARITY FORMATION IN THE RAYLEIGH-TAYLOR PROBLEM

In this section, for certain initially analytic $z(\zeta,0)$ (hence $f(\zeta,0)$) and $W(\zeta,0)$, we give analytical evidence to suggest the instantaneous formation of one or more singularities in $f(\zeta,t)$ and $W(\zeta,t)$ in the unphysical domain $|\zeta| > 1$ at certain points that depend on properties of $z(\zeta,0)$ and $W(\zeta,0)$ in $|\zeta| > 1$.

First, note that, for $0 < t << 1$, we can try a regular perturbation expansion in t. It is clear from (2.18) and (2.26) that

$$y_1(\zeta,t) = y_1(\zeta,0) + t\left[\{R_3(\zeta,0)+R_2(\zeta,0)y_1(\zeta,0)\}\,y_{1\zeta}(\zeta,0) + \zeta y_1(\zeta,0)y_2(\zeta,0)R_1(\zeta,0) + 1 - [1+\zeta I_{1\zeta}(\zeta,0)]y_2(\zeta,0)]\right] + O(t^2) \tag{4.1}$$

$$\frac{1}{\zeta y_2} = \frac{1}{\zeta y_2(\zeta,0)} + t\left[\left\{\frac{R_3(\zeta,0)+R_2(\zeta,0)y_1(\zeta,0)}{\zeta y_2(\zeta,0)}\right\}_\zeta - R_1(\zeta,0)\right] + O(t^2)\,. \tag{4.2}$$

Clearly, since each of $R_1(\zeta,t)$, $R_2(\zeta,t)$, $R_3(\zeta,t)$ and $I_1(\zeta,t)$ involve y_1 and y_2 in the physical domain $\zeta \leq 1$ (where each of them can easily be seen to have a regular perturbation series in t), one will have a regular perturbation expansion in powers of t of these global quantities as well. On substituting into (2.18) and (2.26), the coefficients of all powers of t can be determined, at least in principle.

This regular perturbation series for $t << 1$ becomes disordered when the later terms of the perturbation expansion is more singular than the previous terms, which can occur at some finite ζ_0 or as $\zeta \to \infty$. Here, we will only restrict to breakdown in the power series due to one or more of the following conditions:

(a) $z_\zeta = 0$ at $\zeta = \zeta_0$ with $z_{\zeta\zeta}(\zeta_0,0) \neq 0$, $W_\zeta(\zeta_0,0) \neq 0$

(b) $z_\zeta = 0$ at $\zeta = \zeta_0$ with $z_{\zeta\zeta}(\zeta_0,0) \neq 0$, $W(\zeta,0) = 0$ for all ζ.

(c) As $\zeta \to \infty$, $z_\zeta(\zeta,0) \sim \tilde{b}_2\zeta^{m-1}$ for positive m and $W_\zeta(\zeta,0) \sim \tilde{b}_1\,\zeta^{(n+m-1)}$ for $n \geq 1$.

4a. Birth of a pair of one-half singularities

Here we assume that condition (a) holds at some point ζ_0. In this case, from the definition of f in (2.1) and y_1 and y_2 in (2.16) and (2.17), it follows that the asymptotics of $y_1(\zeta,0)$ and $y_2(\zeta,0)$ as $\zeta \to \zeta_0$ is given by

$$y_1(\zeta,0) \sim \frac{1}{\zeta_0 z_{\zeta\zeta}(\zeta_0,0)(\zeta-\zeta_0)} \tag{4.3}$$

$$y_2(\zeta,0) \sim \frac{W_\zeta(\zeta_0,0)}{\zeta_0 z_{\zeta\zeta}(\zeta_0,0)(\zeta-\zeta_0)}. \tag{4.4}$$

It is clear that the regular perturbation expansion in (4.1) and (4.2) get disordered as $\zeta \to \zeta_0$ for any $t > 0$. Indeed the coefficient of t in (4.1) and (4.2) become the same order as the leading order terms when $\zeta - \zeta_0 = O(t^{1/2})$. This suggests the choice of

$$\eta = \frac{(1-\zeta/\zeta_0)}{t^{1/2}} \tag{4.5}$$

as the inner variable. In the limit $t \to 0^+$ with $\eta = O(1)$, one then finds from (2.18) and (2.26) that the solution is given in the similarity form

$$y_1 = a^{-1}\, t^{-1/2}\, Y_1(\eta) \tag{4.6}$$

$$y_2 = t^{-1/2}\, Y_1(\eta) \tag{4.7}$$

where

$$a = \frac{R_2(\zeta_0,0)}{\zeta_0} \tag{4.8}$$

with a assumed nonzero. With $O(t^{1/2})$ error, each of Y_1 and Y_2 satisfy

$$Y_1 + \eta Y_1' - 2Y_1 Y_1' = 0 \tag{4.9}$$

$$Y_2 + \eta Y_2' + 2Y_2 Y_1' - 2Y_1 Y_2' = 0\,. \tag{4.10}$$

The asymptotic matching condition that (4.6) and (4.7) match to the initial condition that behave like (4.3) and (4.4) near the singular point implies that we must require that for large $|\eta|$

$$Y_1(\eta) \sim \frac{ab}{\eta} \tag{4.11}$$

$$Y_2(\eta) \sim \frac{c}{\eta} \tag{4.12}$$

where

$$b = -\frac{W_\zeta(\zeta_0, 0)}{\zeta_0 f_{\zeta\zeta}(\zeta_0, 0) + f_\zeta(\zeta_0, 0)} \tag{4.13}$$

and

$$c = -\frac{1}{\zeta_0^2 f_{\zeta\zeta}(\zeta_0, 0) + \zeta_0 f_\zeta(\zeta_0, 0)}. \tag{4.14}$$

Equation (4.9) and (4.10) with conditions (4.11) and (4.12) can be solved exactly

$$Y_1(\eta) = \frac{\eta}{2} - \sqrt{\frac{\eta^2}{4} - ba} \tag{4.15}$$

$$Y_2(\eta) = \frac{c}{4b^2a^2}\sqrt{\eta^2 - 4ba}[\eta - \sqrt{\eta^2 - 4ba}]^2. \tag{4.16}$$

The above solutions (4.15), (4.16) show that two square root singularities at $\eta = \pm\sqrt{4ba}$, i.e. at $\zeta = \zeta_0 \mp \zeta_0\sqrt{4bat}$ for $0 < t << 1$ for each of $y_1(\zeta, t)$ and $y_2(\zeta, t)$, each of which is consistent with the expansion (3.13) and (3.14) for sufficiently small $|\zeta_0 \mp \zeta_0\sqrt{4bat}|$. Going to the definition (4.6) and (4.7), it is clear that for $t << 1$, each of $A_1(t)$, $A_2(t)$, $B_2(t)$ are directly determinable from (4.15) and (4.16) at each singularity.

4b. Singularities involving logarithms

Here, we assume condition (b) at some point ζ_0. With this initial condition, clearly from definition of y_1 and y_2 in terms of W and f_ζ, $y_1 = 0$ and $y_2(\zeta, 0)$ has an initial simple pole at $\zeta = \zeta_0$. In this case, it is appropriate to introduce the inner variable

$$\eta = \frac{1}{\sqrt{ab}}[1 - \frac{\zeta}{\zeta_0}]/t \tag{4.17}$$

$$Y_1(\eta, t) = \sqrt{\frac{a}{b}}y_1(\zeta(\eta, t), t) \tag{4.18}$$

$$Y_2(\eta, t) = \sqrt{\frac{a}{b}}t y_2(\zeta(\eta, t), t) \tag{4.19}$$

where

$$a = y_2(1/\zeta_0, 0) = \frac{R_2(\zeta_0, 0)}{\zeta_0} \tag{4.20}$$

$$b = -\frac{1}{\zeta_0 f_\zeta(\zeta_0, 0) + \zeta_0^2 f_{\zeta\zeta}(\zeta_0, 0)}. \tag{4.21}$$

On substituting (4.18) and (4.19) into (2.18) and (2.26), it is clear that for $\eta = O(1)$ and $t << 1$, with $O(t)$ error, we can write

$$-\eta Y_1' + Y_1 Y_1' = -Y_2 \tag{4.22}$$

$$Y_2'[\eta - Y_1] + Y_2[1 + Y_1'] = 0 \tag{4.23}$$

where the prime denotes derivative with respect to η. Now to match to the initial condition, it is clear that as $\eta \rightarrow \infty$,

$$Y_2(\eta, t) \sim \frac{1}{\eta} \tag{4.24}$$

$$Y_1(\eta, t) \sim -\frac{1}{\eta}. \tag{4.25}$$

Since the boundary conditions and the leading order equations do not involve t explicitly, to the leading order for $t << 1$, each of Y_1 and Y_2 will be purely a function of η. We can write the solution down implicitly as

$$\eta = \chi^{-1/2} - \frac{1}{2}\int_0^\chi d\chi' \frac{[e^{\chi'/2} - 1]}{\chi'^{3/2}} \tag{4.26}$$

$$Y_2 = \chi^{1/2} e^{\chi/2} \tag{4.27}$$

$$Y_1 = \chi^{-1/2}(1 - e^{\chi/2}) - \frac{1}{2}\int_0^\chi d\chi' \frac{[e^{\chi'/2} - 1]}{\chi'^{3/2}}. \tag{4.28}$$

Since $\eta(\chi)$ is an analytic function and $\eta_\chi \neq 0$ in the finite χ plane except at the origin, it follows from formulae (4.27) and (4.28) that the only singularities of Y_2 and Y_1 are at $\chi = 0$, which corresponds to $\eta = \infty$, and at $\chi = \infty$, where as $Re\ \chi \rightarrow -\infty$, η takes a finite value

$$\eta_0 = -\frac{1}{2}\int_0^{-\infty} d\chi \frac{[e^{\chi/2} - 1]}{\chi^{3/2}}. \tag{4.29}$$

There are two possible values for η_0, depending on the choice of the branch of $\chi^{1/2}$. From numerical integration, we find

$$\eta_0 = \pm 1.2533i. \tag{4.30}$$

These two points are the only singularities of $Y_1(\eta)$ and $Y_2(\eta)$ in the finite η plane. Note that if $Re\ \chi \rightarrow \infty$, then $\eta \rightarrow \infty$ and so at $\eta = \infty$, there are other possible behaviors, besides (4.24) and (4.25). However, this behavior occurs in the other branch sheet of the Riemann surface generated by the branch points η_0 (given by (4.29)). To deduce the nature of the singularity of Y_1 and Y_2 near $\eta = \eta_0$, we notice that

$$\chi \sim 2ln\ (\eta - \eta_0) + 3ln\ ln(\eta - \eta_0) + .. \tag{4.31}$$

so that for $\eta \rightarrow \eta_0$,

$$Y_1 \sim \eta_0 - (\eta - \eta_0)\ ln\ (\eta - \eta_0) + .. \tag{4.32}$$

$$Y_2 \sim \frac{1}{2}(\eta - \eta_0)[2\ ln\ (\eta - \eta_0)]^2 .. \quad . \tag{4.33}$$

These singularities at specific η_0 correspond to moving singularities in the ζ plane at $\zeta_0 - \sqrt{ab}\zeta_0\eta_0 t$, as can deduced from (4.17). These singularity locations can be expected to be accurate only for $t << 1$, because of the limitation of our analysis.

4c. One-half singularity birth at infinity

We now assume condition (c) holds. We will show that this results in the birth of a one-half singularity at infinity.

From given conditions for case (c), we get

$$y_1(\zeta, 0) \sim b_1 \zeta^n \tag{4.34}$$

$$y_2(\zeta, 0) \sim b_2 \zeta^{-m} \tag{4.35}$$

for some constants b_1 and b_2 with $n \geq 1$ and $m \geq 0$. In this case, we find that the regular perturbation expansion in powers of t break down for ζ so large that $\zeta\, t^{1/n} = O(1)$ or larger. Hence, it is appropriate to introduce an inner variable

$$\eta = \zeta t^{1/n}. \tag{4.36}$$

Then upon substituting

$$y_1(\zeta(\eta, t), t) = \frac{1}{t}\, Y_1(\eta, t) \tag{4.37}$$

$$y_2(\zeta(\eta, t), t) = t^{m/n}\, Y_2(\eta, t) \tag{4.38}$$

into equations (2.18) and (2.26) with $\eta = O(1)$ and $t << 1$, we obtain the following relations (with $O(t)$ error):

$$-Y_1 + \frac{\eta}{n} Y_1' - \eta Y_1 Y_1' = 0 \tag{4.39}$$

$$Y_2'[Y_1 - \frac{1}{n}] - Y_2\, [Y_1' + \frac{m}{n\eta}] = 0 \tag{4.40}$$

where the prime denotes derivative with respect to η keeping t fixed. The initial conditions (4.34) and (4.35), translate to the following equation for $\eta \to 0$

$$Y_1(\eta) \sim b_1 \eta^n \tag{4.41}$$

$$Y_2(\eta) \sim b_2 \eta^{-m}. \tag{4.42}$$

The solution to (4.39) and (4.40) that matches with the asymptotic conditions (4.41), (4.42) is given implicitly as

$$\eta = \left(\frac{Y_1}{b_1}\right)^{1/n} e^{-Y_1} \tag{4.43}$$

$$Y_2 = b_1^{m/n} b_2 Y_1^{-m/n}[1 - nY_1]\,. \tag{4.44}$$

From (4.43), it is clear that η is a regular function of Y_1 everywhere in the finite complex Y_1 plane except at the origin. Further, it is clear that $\frac{d\eta}{dY_1}$ has a simple zero at $Y_1 = \frac{1}{n}$. Thus, it is clear that the only singularity(ies) of Y_1 in the finite η domain (other than $\eta = 0$) is located where

$$\eta_0 = \left(\frac{1}{b_1 n}\right)^{1/n} e^{-1/n}\,. \tag{4.45}$$

Note that this corresponds to n distinct locations corresponding to n distinct branches in (4.45). The behavior of Y_1 and Y_2 near such an η_0 is clearly

$$Y_1 \sim \frac{1}{n} - \sqrt{-2n^{1/n-1} b_1^{1/n} e^{1/n}}(\eta - \eta_0)^{1/2} \; + \; .. \quad . \tag{4.46}$$

From (4.44), it follows that

$$Y_2 \;\sim\; b_1^{m/n} b_2 n^{m/n+1} \sqrt{-2n^{1/n-1} b_1^{1/n} e^{1/n}}(\eta - \eta_0)^{1/2} \; + \; .. \quad . \tag{4.47}$$

Thus, in the case when $m \geq 0$ and $n \geq 1$, there is instantaneous generation of n 1/2 singularity(ies) at ∞ that move into the finite ζ plane. The behavior of y_1 and y_2 at each singularity is clearly seen to be consistent with (3.13) and (3.14). We find that for $t << 1$,

$$\zeta_s(t) = t^{-1/n}\eta_0 \tag{4.48}$$

$$A_1(t) = \frac{1}{nt} \tag{4.49}$$

$$A_2(t) = t^{\frac{1}{2n}-1}\sqrt{-2n^{1/n-1} b_1^{1/n} e^{1/n}} \tag{4.50}$$

$$B_2(t) = \sim \;\; t^{\frac{m}{n}+\frac{1}{2n}} \; b_1^{m/n} b_2 n^{m/n+1} \sqrt{-2n^{1/n-1} b_1^{1/n} e^{1/n}}\,. \tag{4.51}$$

5. NUMERICAL CALCULATIONS AND RESULTS

So far, our numerical calculations have been limited to initial conditions of the special form

$$f(\zeta, 0) = 0 \tag{5.1}$$

$$W(\zeta, 0) = -\epsilon\zeta\,. \tag{5.2}$$

This corresponds to a sinusoidal perturbation in the vortex sheet strength at an initially flat interface. It is likely that the numerical procedure described below can be generalized to other cases; however, our primary motivation in this calculation was to see if indeed the

approach of a one-half singularity as (3.13) and (3.14) towards $|\zeta| = 1$ corresponds to a spike at the physical interface and illustrate through a simple example how the unphysical domain calculation allows us to extract all the relevant information about such a singularity. We chose this special initial condition for simplicity. Further, we only studied the details for $\epsilon = 0.1$, although we checked to see that similar qualitative features appeared for other ϵ. From the analytical evidence presented in Section 4c, one can expect only one singularity forming at ∞, which according to (4.37) and (4.46) will start moving down the negative real ζ axis towards $\zeta = -1$. This is confirmed by the numerical results presented here.

We use the unphysical equations in the form (2.29), (2.32) and (2.33). The variables which are advanced in time are the the 6 N complex point values of $\zeta(\xi,t)$, $\frac{1}{\zeta \dot{y}_2}$ and $\frac{y_1}{\zeta \dot{y}_2}$ at N uniformly spaced out points on each of two circles in the ξ-plane centered at the origin of fixed radii ρ_0 and ρ_1, where $1 < \rho_1 < \rho_0$. These set of $2N$ points in the ξ plane will henceforth be referred to as collocation points. N, chosen between 64 and 256 in all the calculations presented, is taken to be a power of 2 to allow convenience of fast Fourier Transform.

We now describe the step by step procedure to determine the right hand side of (2.29), (2.32) and (2.33) at the collocation points at any time t once $\zeta(\xi,t)$, $\frac{1}{\zeta \dot{y}_2}$ and $\frac{y_1}{\zeta \dot{y}_2}$ are known at these points. This lets us advance these variables in time, using a standard ordinary differential equations solver.

Step 1:

From the known point values of ζ we use a fast Fourier Transform in $Arg\ \xi$ to compute the derivative ζ_ξ at the collocation points. We then evaluate $y_1(\zeta(\xi,t),t)$ and $y_2(\zeta(\xi,t),t)$, using the relation (2.27) and (2.28) at each collocation point.

Step 2:

Assuming that the image $\zeta(\xi,t)$ of $|\xi| = \rho_1$ is outside the unit ζ circle and that each of y_1 and y_2 are analytic functions of ζ on and inside this curve (assumptions checked aposteriori), we obtain

$$y_1(\zeta_0,t) = \frac{1}{2\pi i} \oint_{|\xi|=\rho_1} \frac{y_1(\zeta(\xi,t),t)\zeta_\xi(\xi,t)}{\zeta(\xi) - \zeta_0} \tag{5.3}$$

$$y_2(\zeta_0,t) = \frac{1}{2\pi i} \oint_{|\xi|=\rho_1} \frac{y_2(\zeta(\xi,t),t)\zeta_\xi(\xi,t)}{\zeta(\xi) - \zeta_0} \tag{5.4}$$

$$y_{1\zeta}(\zeta_0,t) = \frac{1}{2\pi i} \oint_{|\xi|=\rho_1} \frac{y_1(\zeta(\xi,t),t)\zeta_\xi(\xi,t)}{[\zeta(\xi) - \zeta_0]^2}. \tag{5.5}$$

We compute $y_1(e^{i\nu},t)$ and $y_2(e^{i\nu},t)$ for N uniformly spaced out ν in the real interval $(0,2\pi)$. The integrals in (5.3)-(5.5) were implemented by using a real angular variable $\hat{\nu}$ in

the representation $\xi = \rho_1\ e^{i\hat{\nu}}$ and then using a trapezoidal rule that uses the N uniformly spaced points in $\hat{\nu}$ over the interval $(0,\ 2\ \pi)$.

Step 3:

Using the computation in Step 2, $Re[y_1\ y_2^*]$ and $\frac{1}{2}|y_1|^2$ are computed at N uniformly spaced out points on $|\zeta| = 1$ circle which is then used to compute c_j and $\tilde{c}_j$ (for $0 \leq j \leq N/2$) in the Fourier representations

$$Re[y_1(e^{i\nu},t)y_2^*(e^{i\nu},t)] = \sum_{j=-\infty}^{\infty} c_j\ e^{ij\nu} \tag{5.6}$$

$$-\frac{1}{2}|y_1(e^{i\nu},t)|^2 = \sum_{j=-\infty}^{\infty} \tilde{c}_j\ e^{ij\nu}\,. \tag{5.7}$$

This is then used to calculate $R_3(\zeta(\xi,t),t)$ and $I_{1_\zeta}(\zeta(\xi,t),t)$ at the collocation points by using the representations

$$R_3(\zeta,t) = -c_0\zeta - 2\sum_{j=1}^{\infty} c_j\zeta^{1-j} \tag{5.8}$$

$$I_{1_\zeta}(\zeta,t) = 2\sum_{j=1}^{\infty} j\tilde{c}_j\zeta^{-j-1} \tag{5.9}$$

that follow from (2.11), (2.15) and (2.22).

Step 4:

Using (5.3)-(5.5) and taking $\zeta_0 = \frac{1}{\zeta(\xi,t)}$ for each of the collocation points, we compute R_2 and R_{1_ζ} by using (2.20) and (2.21).

Once steps 1 through 4 are implemented, we are in a position to evaluate the right hand side of (2.29), (2.32) and (2.33) at the collocation points. This allows us to advance each of ζ, $\frac{1}{\zeta\hat{y}_2}$ and $\frac{\hat{y}_1}{\zeta\hat{y}_2}$ in time by using a standard ordinary differential equations solver. We monitored the computed values of $|\zeta(\xi,t)|$ at the collocation points to make sure that they were outside the unit circle, or otherwise (5.3)-(5.5) will not be valid. Further, when $|\zeta| < 1.04$, we discontinued calculations since accurate evaluation of the integrals in (5.3)-(5.5) required a value of N larger than 256, the largest value we allowed in our calculation.

As a biproduct of the above calculation, we get the physical interface location since the knowledge of $y_2(\zeta,t)$ on the unit circle gained in Step 2 allows us to reconstruct (up to a time dependent constant) the conformal mapping function $z(\zeta,t)$ on $|\zeta| = 1$ since

$$z(e^{i\nu},t) = z(1,t) + \int_0^{\nu} d\nu \frac{1}{y_2(e^{i\nu'},t)}\,. \tag{5.10}$$

Note that $z(1,t)$ cannot be found from the unphysical equations since y_1 and y_2 involve the derivative z_ζ. However, for any symmetric initial condition, $z(1,t)$ is purely imaginary.

It is well known that the average height (in the physical z domain) $\frac{1}{2\pi}\int_0^{2\pi} y dx$ is conserved in time and so

$$\int_0^{2\pi} d\nu \; Im \; z(e^{i\nu},t) \; Re \; z_\nu(e^{i\nu},t) = \int_0^{2\pi} d\nu \; Im \; z(e^{i\nu},0) \; Re \; z_\nu(e^{i\nu},0). \tag{5.11}$$

Since $z(\zeta,0)$ is known initially, (5.11) can be used to compute $z(1,t)$ in (5.10), which allows us to compute $z(e^{i\nu},t)$ completely. For purposes of computing the integrals in (5.10), (5.11), we used a trapezoidal rule using the N uniformly spaced out points on the unit ζ circle, where y_2 is known.

We also computed the following integrals using a trapezoidal rule and the values of the functions at the collocation points

$$N_0 = \frac{1}{2\pi i}\oint_{|\xi|=\rho_0} d\xi \frac{\zeta_{\xi\xi}}{\zeta_\xi} - \frac{1}{2\pi i}\oint_{|\xi|=\rho_1} d\xi \frac{\zeta_{\xi\xi}}{\zeta_\xi} \tag{5.12}$$

$$\xi_0 = \frac{1}{2\pi i}\oint_{|\xi|=\rho_0} d\xi \frac{\xi\zeta_{\xi\xi}}{\zeta_\xi} - \frac{1}{2\pi i}\oint_{|\xi|=\rho_1} d\xi \frac{\xi\zeta_{\xi\xi}}{\zeta_\xi} \tag{5.13}$$

$$\zeta_s = \frac{1}{2\pi i}\oint_{|\xi|=\rho_0} d\xi \frac{\zeta\zeta_{\xi\xi}}{\zeta_\xi} - \frac{1}{2\pi i}\oint_{|\xi|=\rho_1} d\xi \frac{\zeta\zeta_{\xi\xi}}{\zeta_\xi} \tag{5.14}$$

$$z_0 = \frac{1}{2\pi i}\oint_{|\xi|=\rho_0} d\xi \frac{\zeta_{\xi\xi}^2}{\zeta_\xi} - \frac{1}{2\pi i}\oint_{|\xi|=\rho_1} d\xi \frac{\zeta_{\xi\xi}^2}{\zeta_\xi} \tag{5.15}$$

$$\hat{A}_1 = \frac{1}{2\pi i}\oint_{|\xi|=\rho_0} d\xi \frac{\hat{y}_1\zeta_{\xi\xi}}{\zeta_\xi} - \frac{1}{2\pi i}\oint_{|\xi|=\rho_1} d\xi \frac{\hat{y}_1\zeta_{\xi\xi}}{\zeta_\xi} \tag{5.16}$$

$$\hat{A}_2 = \frac{1}{2\pi i}\oint_{|\xi|=\rho_0} d\xi \frac{\hat{y}_{1_\xi}\zeta_{\xi\xi}}{\zeta_\xi} - \frac{1}{2\pi i}\oint_{|\xi|=\rho_1} d\xi \frac{\hat{y}_{1_\xi}\zeta_{\xi\xi}}{\zeta_\xi} \tag{5.17}$$

$$\hat{B}_2 = \frac{1}{2\pi i}\oint_{|\xi|=\rho_0} d\xi \frac{\hat{y}_2\zeta_{\xi\xi}}{\zeta_\xi} - \frac{1}{2\pi i}\oint_{|\xi|=\rho_1} d\xi \frac{\hat{y}_2\zeta_{\xi\xi}}{\zeta_\xi}. \tag{5.18}$$

Here $\zeta_{\xi\xi}$ is obtained at the collocation points through fast Fourier transforming ζ as a function of $Arg\ \xi$ on $|\xi| = \rho_0$ and $|\xi| = \rho_1$.

It was observed that for t small enough, all the integrals (5.12)-(5.18) were zero up to numerical accuracy (five digits in the worst case presented here), as must be the case if there is no singularity of the integrands within the annular region in the ξ plane between $|\xi| = \rho_0$ and $|\xi| = \rho_1$. Then, after some time, which was found to depend on the choice of ρ_0, the value of N_0 changed dramatically over a short period of time before settling down to a value of 1 (up to five digits). The transient time when N_0 was significantly different from 0 or 1 became progressively shorter as N was increased. We interpreted this result to mean that around this time, a zero $\xi_0(t)$ of ζ_ξ crossed from $|\xi| > \rho_0$ into the

region $|\xi| < \rho_0$. The dependence of the results on N is not expected as the numerical quadrature is not adequate during the short period of time when $\xi_0(t)$ is very close to $|\xi| = \rho_0$. Note however, this inaccuracy has no impact on the actual solutions to (2.29), (2.32) and (2.33) since it was found that the right-hand sides of (2.29), (2.32) and (2.33) were well behaved when this happened. This is not unexpected since there is no division by ζ_ξ in implementing steps 1 through 4, as necessary to calculate the integrals (5.12)-(5.18). Figures 3 and 4 show the images of 256 uniformly spaced out points on $|\xi| = \rho_0 = 5$, at $t = 1.4$ and $t = 1.6$, just before and after N_0 changed its value from 0 to 1. At $t = 1.4$, the zero of ζ_ξ is at $\xi_0 = -5.295$ and the corresponding ζ_s (singularity location in the ζ plane) is at -2.061. The apparent cusp in Fig. 3 is because ζ_ξ is close to 0 at $\xi = -5$ due to the proximity of ξ_0. At a slightly later time when ξ_0 is exactly -5, we get a true cusp. The image of $|\xi| = 5$ in the ζ plane at $t = 1.6$ clearly shows that the curve is not simple and that it intersects itself. We clearly see that the failure of one to one correspondence of ξ and ζ on this curve. Relating the geometric nature of the observed image in Fig. 4 to general mapping properties of an analytic function, it is clear that there is a zero of ζ_ξ in $|\xi| < \rho_0$, as is consistent with the computed value of $N_0 = 1$ at this time. We also monitored the image of $|\xi| = \rho_1$ and it was found that throughout our calculations, its image consisted of a simple curve completely outside $|\zeta| = 1$. Figure 5 shows the image of 256 points on $|\xi| = \rho_1 = 1.5$ under $\zeta(\xi, t)$ at $t = 2.4$. Another property that was apparent in our calculations is that the image under $\zeta(\xi, t)$ had the effect of moving points both radially outwards and tangentially away from $\zeta = 1$, which corresponds to the bubble part of the interface, while points tended to move both radially inwards and slide tangentially towards $\zeta = -1$, which corresponds to the upward moving spike (recall gravity is upwards) in the physical domain. This tendency is clear in Figures 3-5. There are a lot more points near the negative real ζ axis than the positive ζ axis, even when all the points were initially uniformly spaced out on a circle centered about the origin. Furthermore, the points near $\zeta = -1$ have moved closer while image points near $\zeta = 1$ are further away than they were initially (Recalling $\zeta(\xi, 0) = \xi$). Since the image $\zeta(\xi, t)$ defines the motion of characteristic, it is clear that information from the unphysical plane tends to flow towards a spike that will make the spike features sensitive to small changes in specified initial conditions in the physical domain $|\zeta| \leq 1$. Near the bubble however, the opposite will be true. Further implications of this property will be discussed in Section 7.

From the calculus of residues, it follows that for $\zeta(\xi, t)$, analytic in ξ, when a zero of ζ_ξ is in the annular region the computed ξ_0 in (5.13) is indeed the location $\xi_0(t)$ of the zero of ζ_ξ. Further, the value in (5.14) will be the corresponding image $\zeta_s(t)$ in the ζ plane. The value z_0 in (5.15) is clearly $\zeta_{\xi\xi}(\xi_0)$. Further, the computed $\hat{A}_1$, $\hat{A}_2$ and $\hat{B}_2$

in (5.16)-(5.18) has to correspond to to $\hat{y}_1(\xi_0,t)$, $\hat{y}_{1\xi}(\xi_0,t)$ and $\hat{y}_2(\xi_0,t)$. Whenever the calculated $N_0 = 1$, the relations (3.15)-(3.17) are used to compute A_1, A_2 and B_2 in the expansion (3.13)-(3.14). The calculation had to be discontinued when any of the following conditions occurred

(i) The image of any of the collocation points on $\zeta(\xi,t)$ for $|\xi| = \rho_1$ was in $|\zeta| < 1.04$ since this made it difficult to get a sufficiently accurate result in the quadratures (5.3)-(5.5) for N not exceeding 256.

(ii) The image of any collocation points on $|\xi| = \rho_0$ under the computed $\zeta(\xi,t)$ came inside the unit ζ circle as this made the evaluation in (5.8) and (5.9) sensitive to the small errors in c_j and $\tilde{c}_j$.

(iii) Whenever $|\xi_0|$ computed in (5.12) was smaller that ρ_1, as otherwise we could not ensure that the singularity $\zeta_s(t)$ was outside the image of $|\xi| = \rho_1$ in the ζ plane, as necessary for (5.3)-(5.5) to be valid.

Since we were interested in tracking the singularity, the choice of ρ_0 and ρ_1 in our calculations was dictated by the necessity that the calculations could be carried out over a significant interval of time for which N_0 was nonzero and none of the conditions (i)-(iii) resulted. For all the calculations reported in the table below, we used $\rho_1 = 1.5$, though we changed ρ_1 between 1.25 and 2 to ascertain that the calculations of the physical interface did not depend on the choice of ρ_1 as would be the case if the image of $|\xi| = \rho_1$ in the ζ plane did not contain any singularity of $y_1(\zeta,t)$ and $y_2(\zeta,t)$. The interfacial location also agreed with a standard physical domain code based on satisfying (2.8) and (2.12) at uniformly spaced out points on the unit ζ circle, with f and W having a truncated representation of (2.2) and (2.3). This helped us further confirm that there was indeed no singularity of y_1 and y_2 for $|\zeta| < |\zeta_s|$. We also ensured that the values of the integrals in (5.12)-(5.18) at any time t were independent of ρ_1 when N_0 had settled to the value 1. The value of ρ_0 was varied from a maximum of 50 to a minimum of 3.0 in order to track the singularity at various stages of its motion. For a large value of ρ_0, the value of N_0 settled to a value of 1 at a relatively small t. However, in such cases the computation could not be carried out for a long time because of the limitation of condition (ii) cited above. In that case, one or more points on the secondary lobe (as in Fig. 4) of the image of $|\xi| = \rho_0$ tended to move in into $|\zeta| < 1$ before long. For smaller values of ρ_0 in the range we tried, computation could be carried out for a significantly longer time; however for such cases, singularity tracking was not possible for earlier times since $\xi_0(t)$ was then outside $|\xi| = \rho_0$. However, smaller ρ_0 allowed us to track ζ_s in the later stages when ζ_s was getting fairly close to -1 when the corresponding interface shape near $\zeta = -1$ showed a developing spike. We also noted that for two different ρ_0, in the overlapping time interval when the

computed N_0 had settled to a value of 1, there was agreement in the computations (5.12)-(5.18). This provided an additional check on the code and on our assumption that there was indeed only one singularity in this case.

Table 1 lists the various quantities of interest as a function of time. The results have been checked by appropriately doubling N until there was no variation in the results. With the limited number of $N \leq 256$, we had difficulty ensuring desirable accuracy for t greater than 2.4. The physical interface at $t = 2.4$ is shown in Fig. 6. The image of $\zeta = -1$ corresponds to the spike observed at $x = \pi$. The curve marked 1 in figures 7, 8, 9, 10 show ζ_s, A_1, A_2 and B_2 as a function of t, where we used (3.15)-(3.17) and the computed quantities in (5.12)-(5.18). The curve marked 2 is the analytic prediction (4.48)-(4.51), where $b_1 = -\epsilon = -0.1$, $b_2 = 1$, $n = 1$ and $m = 0$. Since the theory in Section 4 requires $t << 1$, we get surprisingly good agreement even for t not all that small. Figure 11 shows $Im\ z(1,t)$ and $Im\ z(-1,t)$, the vertical location of the bubble tip and spike respectively. Though, the spike does not appear very well developed in Fig. 6, Fig. 11 shows that that the long time asymptotic range has been reached where the spike accelerates upwards (the direction of gravity) with the acceleration approaching free fall. Fig. 12 shows the product $Re[A_2\ B_2^*]$ as a function of time. In this case, since each of A_2 and B_2 are real, $Re\ [A_2 B_2^*] = A_2 B_2$. This quantity appears to reach a minimum and then increase. Thus $M_1(t)$, as defined in (6.32), goes through a maximum and then decreases. We take this as an indication that $M_1(t)$ does not blow up in finite time. We cannot rule out the possibility that the observed trend in $M_1(t)$ reverses at at an even longer time; but given that the spike has reached its asymptotic acceleration towards the the end of our calculations, we do not expect this to happen. In the following section, analytical evidence will be presented to show that under the assumption that $\int_{t_0}^{t} M_1(t)dt$ does not blow up in finite time, an isolated one-half singularity of the type (3.13) and (3.14) cannot reach the physical domain $|\zeta| = 1$ in finite time.

6. EVENTUAL FATE OF A ONE-HALF SINGULARITY

We now want to understand the fate of an isolated singularity of the type given by (3.13) and (3.14), once it is already close to the unit circle in the ζ plane.

Note that (2.21), (2.22) and (3.18) imply that

$$\frac{\dot{\zeta}_s}{\zeta_s} = - I_2(\zeta_s(t),t) - y_2(\frac{1}{\zeta_s(t)},t)\ y_1(\zeta_s(t),t)\,. \tag{6.1}$$

Now, from (2.25), (3.13) and (3.14), it follows that

$$I_2(\zeta_s,t) = \frac{1}{2\pi}\int_0^{2\pi} d\nu \left[\frac{e^{i\nu} + \zeta_s}{e^{i\nu} - \zeta_s}\right] Q(\nu,t) \tag{6.2}$$

where

$$Q(\nu,t) \;=\; Re\;\left[\; y_1^*(e^{i\nu},\;t),t)\;y_2(e^{i\nu},t)\;\right]\;. \tag{6.3}$$

It is convenient to define

$$Q_1(\nu,t) \;=\; Re\;\left[A_1^*(t)\;B_2(t)\;(e^{i\nu}-\zeta_s(t))^{1/2}\;\right] \tag{6.4}$$

$$Q_2(\nu,t) \;=\; Re\;\left[A_1^*(t)\;B_3(t)\;(e^{i\nu}-\zeta_s(t))\;\right] \tag{6.5}$$

$$Q_3(\nu,t) \;=\; Re\;[A_2^*(t)\;B_2(t)]\;|e^{i\nu}\;-\;\zeta_s(t)|\,. \tag{6.6}$$

If we denote

$$\zeta_s \;=\; R\;e^{i\nu_0}\,, \tag{6.7}$$

then for $R \;\rightarrow\; 1^-$, the behavior of $Q(\nu,t)$ in the vicinity of ν_0 is given by

$$Q(\nu,t) \;=\; Q_1(\nu,t) \;+\; Q_2(\nu,t) \;+\; Q_3(\nu,t) \;+\; O(|\nu-\nu_0|^{3/2})\,. \tag{6.8}$$

Now let's define

$$I_{21}(\zeta_s,t) \;=\; \frac{1}{2\pi}\int_0^{2\pi} d\nu\;\left[\frac{e^{i\nu}\;+\;\zeta_s}{e^{i\nu}-\zeta_s}\right]Q_1(\nu,t) \tag{6.9}$$

$$I_{22}(\zeta_s,t) \;=\; \frac{1}{2\pi}\int_0^{2\pi} d\nu\;\left[\frac{e^{i\nu}\;+\;\zeta_s}{e^{i\nu}-\zeta_s}\right]Q_2(\nu,t) \tag{6.10}$$

$$I_{23}(\zeta_s,t) \;=\; \frac{1}{2\pi}\int_0^{2\pi} d\nu\;\left[\frac{e^{i\nu}\;+\;\zeta_s}{e^{i\nu}-\zeta_s}\right]Q_3(\nu,t)\,. \tag{6.11}$$

By changing the integration variable from ν to $-\nu$ in each of (6.9), (6.10) and (6.11), it is not difficult to establish the property that for $1 \;\leq\; j \;\leq\; 3$,

$$I_{2j}(\zeta_s,t) \;=\; -\;\frac{1}{2\pi}\int_0^{2\pi} d\nu\;\left[\frac{e^{i\nu}\;+\;\frac{1}{\zeta_s}}{e^{i\nu}-\frac{1}{\zeta_s}}\right]Q_j(-\nu,t)\,. \tag{6.12}$$

Now note that from previous expressions (6.4), (6.5) and (6.6)

$$Q_1(-\nu,t) \;=\; Re\;\left[A_1(t)\;B_2^*(t)\;(e^{i\nu}-\zeta_s^*(t))^{1/2}\;\right] \tag{6.13}$$

$$Q_2(-\nu,t) \;=\; Re\;\left[A_1(t)\;B_3^*(t)\;(e^{i\nu}-\zeta_s^*(t))\;\right] \tag{6.14}$$

$$Q_3(-\nu,t) \;=\; Re\;[A_2(t)\;B_2^*(t)]\;|e^{i\nu}\;-\;\zeta_s^*(t)|\,. \tag{6.15}$$

Each of (6.13) and (6.14) are clearly seen to be the real part of simple analytic functions for $\zeta \;=\; e^{i\nu}$. Therefore, it immediately follows that

$$I_{21}(\zeta_s(t),t) \;=\; -A_1(t)\;B_2^*(t)\;(\frac{1}{\zeta_s(t)}\;-\;\zeta_s^*(t))^{1/2} \tag{6.16}$$

$$I_{22}(\zeta_s(t),t) \;=\; -A_1(t)\; B_3^*(t)\; (\frac{1}{\zeta_s(t)} \;-\; \zeta_s^*(t)). \tag{6.17}$$

Now consider $I_{23}(\zeta_s(t),t)$. From (6.6) and (6.11), it follows that

$$I_{23}(\zeta_s(t),t) \;=\; -\frac{1}{2\pi}\; Re\;[A_2^*(t)\; B_2(t)] \;\int_0^{2\pi} d\nu \;\; |e^{i\nu} \;-\; \zeta_s^*(t)| \;\left[\frac{e^{i\nu} \;+\; \frac{1}{\zeta_s(t)}}{e^{i\nu} \;-\; \frac{1}{\zeta_s(t)}}\right]. \tag{6.18}$$

Using (6.7) and periodicity and symmetry of the integrand, it follows that

$$I_{23}(\zeta_s(t),t) \;=\; -\frac{(R^2-1)}{\pi}\; Re\;[A_2^*(t)\; B_2(t)] \;\int_0^{\pi} \frac{d\nu}{(R^2 \;+\; 1 \;-\; 2\; R\; cos\nu)^{1/2}}. \tag{6.19}$$

Now we want to consider the asymptotics of (6.19) in the limit $R \;\rightarrow\; 1^-$. To do this it is convenient to break the integral range in (6.19)

$$\int_0^{\pi} \;=\; \int_{\epsilon}^{\pi} \;+\; \int_0^{\epsilon} \tag{6.20}$$

where $1 \;>>\; \epsilon \;>>\; (R-1)$. For the first integral in (6.20), the leading order asymptotics can be found by replacing R by 1. For the second integral in (6.20), the leading order asymptotics can be found by first simplifying the $cos\;\nu$ by $1 \;-\; \frac{1}{2}\;\nu^2$ and then replacing the integration variable ν by $\tilde{\nu}$, where $\nu \;=\; (R-1)\;\tilde{\nu}$. One then finds the leading order asymptotics of (6.19) as

$$I_{23}(\zeta_s(t),t) \;\sim\; -2\;\frac{R-1}{\pi}\; Re\;(A_2^* B_2)\;\left[\int_{\epsilon}^{\pi} \frac{d\nu}{2\;sin\;\frac{1}{2}\;\nu} \;+\; \int_0^{\epsilon/(R-1)} \frac{d\tilde{\nu}}{(1 \;+\; \tilde{\nu}^2)^{1/2}}\right]. \tag{6.21}$$

Each of these integrals can be computed exactly with ϵ dropping out completely on addition. We find

$$I_{23}(\zeta_s(t),t) \;=\; -2\;\frac{(R-1)}{\pi}\; Re\;(A_2^*(t)\; B_2(t))\;[3\;ln\;2 \;-\; ln\;(R-1) \;\;+\; o(1)\;]. \tag{6.22}$$

Now let compute

$$I_R(\zeta_s(t),t) \;\equiv\; I_2(\zeta_s(t),t) \;-\; I_{21}(\zeta_s(t),t) \;-\; I_{22}(\zeta_s(t),t) \;-\; I_{23}(\zeta_s(t),t). \tag{6.23}$$

It is clear that

$$I_R(\zeta_s(t),t) \;=\; \frac{1}{2\pi}\;\int_0^{2\pi} d\nu\;\left[\frac{e^{i\nu} \;+\; \zeta_s}{e^{i\nu} - \zeta_s}\right] Q_R(\nu,t) \tag{6.24}$$

where

$$Q_R(\nu,t) \;\equiv\; Q(\nu,t) \;-\; Q_1(\nu,t) \;-\; Q_2(\nu,t) \;-\; Q_3(\nu,t). \tag{6.25}$$

This can also be written as

$$I_R(\zeta_s(t),t) \;=\; \frac{1}{2\pi}\int_0^{2\pi} d\nu\;\left[\frac{-R^2+1-2iRsin(\nu-\nu_0)}{1+R^2-2Rcos(\nu-\nu_0)}\right]\;Q_R(\nu,t)\,. \tag{6.26}$$

As $R \rightarrow 1^-$, the above expression reduces to

$$I_R(\zeta_s(t),t) \;=\; -\frac{R-1}{\pi}\int_0^{2\pi} d\nu\;\frac{Q_{R_0}(\nu,t)}{2-2cos(\nu-\nu_0)}\;[1\;+\;o(1)]$$

$$-\;\frac{i}{2\pi}\int_0^{2\pi} d\nu\;\;cot\;\frac{1}{2}\,(\nu-\nu_0)\;\;\;Q_{R_0}(\nu,t)\;[1\;+\;o(1)\,] \tag{6.27}$$

where the subscript 0 in Q_R refers to its evaluation with $\zeta_s = e^{i\nu_0}$. Notice that from the behavior (6.8), each of the integrals in (6.27) exists.

Now note the fact that if for any complex ζ_s singularity, near which the asymptotic behavior of y_1 and y_2 is given by (3.13) and (3.14), there is a singularity at ζ_s^* in the neighborhood of which

$$y_1(\zeta,t) \;=\; A_1^*(t)\;+\;A_2^*(t)\;(\zeta-\zeta_s^*(t))^{1/2}\;+\;A_3^*(t)(\zeta-\zeta_s^*)\;+\;o(\zeta-\zeta_s^*)^{3/2}.. \tag{6.28}$$

and

$$y_2(\zeta,t) \;=\; B_2^*(t)\;(\zeta-\zeta_s^*(t))^{1/2}\;+\;B_3^*(t)(\zeta-\zeta_s^*)\;+\;o((\zeta-\zeta_s^*)^{3/2}).. \quad . \tag{6.29}$$

Now as $R \rightarrow 1^-$, the point $\frac{1}{\zeta}$ comes close to $\zeta = \zeta_s^*$ and so the last term in (6.1) yields

$$-y_2(\frac{1}{\zeta_s(t)},t)\;y_1(\zeta_s(t),\;t)\;\sim\;A_1(t)\;B_2^*\;(\frac{1}{\zeta_s(t)}\;-\;\zeta_s^*(t))^{1/2}$$
$$+\;A_1(t)\;B_3^*\;(\frac{1}{\zeta_s(t)}\;-\;\zeta_s^*(t))\;+\;o(R-1) \tag{6.30}$$

Taking the real part of (6.1), using (6.7), (6.16), (6.17), (6.22), (6.27) and (6.29) in the asymptotic limit $R \rightarrow 1^-$, we get

$$\dot{R} \;=\; M_1(t)\;(R-1)\;ln(R-1)\;+\;M_2(t)\;(R-1)\;+\;o(R-1) \tag{6.31}$$

where

$$M_1(t) \;=\; -\frac{2}{\pi}\;Re\;[A_2^*(t)\;B_2(t)\,] \tag{6.32}$$

$$M_2(t) \;=\; \frac{6\;ln2}{\pi}\;Re\;[A_2^*(t)\;B_2(t)]\;-\;\frac{1}{\pi}\int_0^{2\pi} d\nu\;\frac{Q_{R_0}(\nu,t)}{2-2\;cos\;(\nu-\nu_0)}\,. \tag{6.33}$$

The solution of (6.31) to the leading order is

$$ln\ (R-1)\ =\ ln\ (R_0\ -\ 1)\ e^{\int_{t_0}^{t}\ dt'\ M_1(t')}. \tag{6.33}$$

If we assume that $\int_{t_0}^{t} M_1(t)dt$ does not blow up for any finite time, then it follows from (6.34), that there will be absence of finite time singularity. This assumption is consistent with the results from numerical calculations as reported in the previous section, though for a special initial condition. In that case, recall that $M_1(t)$ actually appeared to decrease after sufficiently long time.

7. DISCUSSIONS AND CONCLUSION

We have analyzed some properties of the unphysical equation derived earlier by Tanveer (1991a). For early times, for a specific class of analytic $W(\zeta,0)$ and $z(\zeta,0)$ in $|\zeta| > 1$ (except possibly at infinity), we noted how one or more singularities can form at a point in $|\zeta| > 1$, where $z_\zeta(\zeta,0)$ is zero. One-half singularities are shown to be generated, though we show that other singularities of a much more complicated form involving logarithms are possible. Further, analytical evidence suggests that one or more one-half singularity may be born at $\zeta = \infty$, which moves to the finite ζ plane instantaneously. The numerical computation, although for a special case, clearly shows that one-half singularities on their approach towards the physical domain corresponds to a continually developing spike. The connection of more complicated singularities with interfacial features is yet to be made. The numerical computation also suggests that the characteristic field in the unphysical plane is pointed away from the bubble and towards the spike. With an assumption that appears to be consistent with the numerical calculation for the special case, our analytical evidence suggests that an isolated one-half singularity of the type given in (3.13) and (3.14) cannot reach the physical domain in finite time. We have not investigated the question of finite time singularity in the physical domain when possibly multiple one-half singularities merge or other forms of singularities are present, and this remains an open question.

It is clear that the location of formation of initial singularities depend on the specifics of the initial conditions $z(\zeta,0)$ and $W(\zeta,0)$ in $|\zeta| > 1$. Clearly, it is possible to make arbitrary small perturbation in the physical domain $|\zeta| \leq 1$ that significantly alters the location and number of singularities that are formed in $|\zeta| > 1$. Further, our numerical computation, though for a special case, appears to indicate that the characteristic field in the unphysical plane is directed away from the bubble and towards the spike. This feature accounts for the sensitivity of spike to initial conditions in the physical plane. Further, if one were to perturb the initial condition (5.1) and (5.2) by placing an additional singularity in $|\zeta| > 1$ that is weak in the sense that its contribution to the right hand side of (2.29)

is small, then the characteristic field generated in this problem will be close to what has been computed in Section 5. Since a singularity moves along with the characteristic field, one can expect that in due time, this additional singularity will also approach $\zeta = -1$, which corresponds to the spike.

This suggests that in a general way, it might be true that weaker singularities have the tendency to merge with stronger ones. If this is generally true, we speculate this as a possible reason why bubble competition results in a dominant bubble. The image under $z(\zeta, t)$ of an arc on $|\zeta| = 1$ between two approaching singularities must contain the bubble region, since each spike possibly corresponds to a singularity. If the singularities merge pairwise in the ζ plane, the corresponding bubble region between these two singularities will disappear resulting in one larger bubble. However, if multiple singularities of nearly equal strength results from an initial condition, this merger can be expected to take a while as the characteristic field will be almost equally affected by all the singularities. The transient dynamics observed in experiment can be expected to depend on the location of initial singularities and their motion, the randomness resulting from the ill-posedness in determining $z(\zeta, 0)$ and $W(\zeta, 0)$ in $|\zeta| > 1$, when they are only given in the physical domain $|\zeta| \leq 1$. Confirmation of this scenario must await further investigations in the future.

Acknowledgement

The author wishes to thank Professors G.R. Baker, P.G. Saffman and Dr. M. Siegel for discussions and suggestions. This work was supported by the National Science Foundation (DMS-9107608).

References

1. Baker, G.R., Caflisch, R. & Siegel, M., 1992, Submitted to the Journal of Fluid Mechanics.

2. Baker,G.R., Meiron,D.I., & Orszag, S.A. 1980 Phys. Fluids 23, p.1485.

3. Baker, G.R., Meiron, D. & Orszag, S., 1982, Generalized vortex methods for free-surface flow problems. J. Fluid Mech., 123:477-501.

4. Caflisch, R. & Orlenna, O., 1989, Singular solutions and ill posedness of vortex sheets, Siam J. Math An., Vol. 20, 2, 293-307.

5. Cowley, S.J., Baker, G.R., Paige, M. & Tanveer, S., To be submitted to J. Fluid Mech.

6. Davies, R.M. & Taylor, G.I. 1950, Proc. R. Soc. London A 200, 375.

7. Emmons, H.W., Chang, C.T. & Watson, B.C. 1959 J. Fluid Mech. 7, p.177.

8. Gardner, C.L., Glimm, J., McBryan, O., Menikoff, R., Sharp, D.H. & Zhang, Q., 1988, The dynamics of bubble growth for Rayleigh-Taylor unstable interfaces, Phys. Fluids, 31, 447.

9. Krasny, R. 1986, J. Comput. Phys. 65, p.292.

10. Moore, D.W. 1979 Proc. R. Soc. Lond. A365, p.105.

11. Moore, D.W. 1985 in Theor. and Appl. Mech., Proc XVI IUTAM.

12. Read, K.I., Physica 12D, p. 45.

13. Sharp, D.H. 1984. An overview of Rayleigh-Taylor instability. Physica D, 12:3-18.

14. Shelley, M.J. 1991 , A study of singularity formation in vortex sheet motion by a spectrally accurate method. To appear in the Journal of Fluid Mechanics.

15. Siegel, M., 1989, An analytical and numerical study of singularity formation in the Rayleigh-Taylor problem. Ph.D thesis, Courant Institute of Mathematical Sciences.

16. Tanveer. S., 1991a, Singularities in Water Wave and the classical Rayleigh-Taylor problem, Proc. Roy. Soc. London A 435, pp 137-158.

17. Tanveer. S., 1991b, Evolution of a Hele-Shaw interface for small surface tension, Submitted to Phil. Trans. Royal Soc. London.

18. Verdon, C.P., McCrory, R.L., Morse, R.L., Baker, G.R., Meiron, D.I. & Orszag, S.A., 1982, Phys. Fluids 25, p. 1653.

t	ξ_0	ζ_s	A_1	A_2	B_2	$Spike$	$Bubble$
0.24	−41.27	−15.20	4.249	−1.541	0.3626	0.024527	−0.023940
0.40	−24.38	−8.994	2.639	−1.244	0.4721	0.041930	−0.040243
0.60	−15.72	−5.820	1.868	−1.095	0.5843	0.065733	−0.061680
0.80	−11.28	−4.201	1.516	−1.046	0.6857	0.092863	−0.084978
1.00	−8.533	−3.209	1.327	−1.048	0.7808	0.12467	−0.11087
1.20	−6.657	−2.539	1.221	−1.083	0.8712	0.16283	−0.14008
1.40	−5.295	−2.061	1.161	−1.142	0.9555	0.20949	−0.17333
1.60	−4.268	−1.711	1.132	−1.220	1.029	0.26745	−0.21131
1.80	−3.477	−1.454	1.126	−1.315	1.085	0.34039	−0.25464
2.00	−2.860	−1.269	1.141	−1.426	1.108	0.43316	−0.30381
2.20	−2.381	−1.141	1.181	−1.559	1.080	0.55200	−0.35913
2.40	−2.013	−1.062	1.248	−1.729	0.9805	0.70441	−0.42066

Table 1: Various parameters characterizing the one-half singularity. The last two columns contain $Im\ z(-1,t)$ and $Im\ z(1,t)$, the vertical locations of the spike and the bubble.

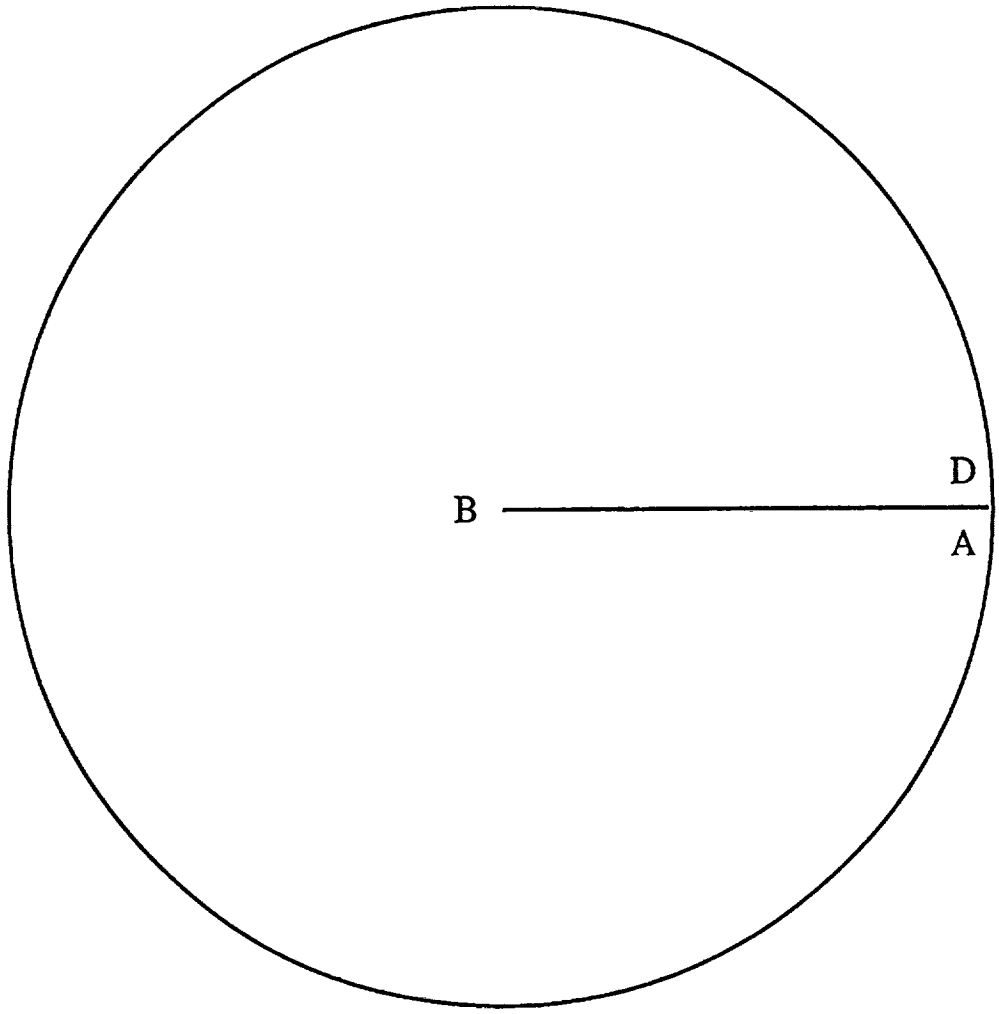

Fig. 1: The complex ζ cut unit circle.

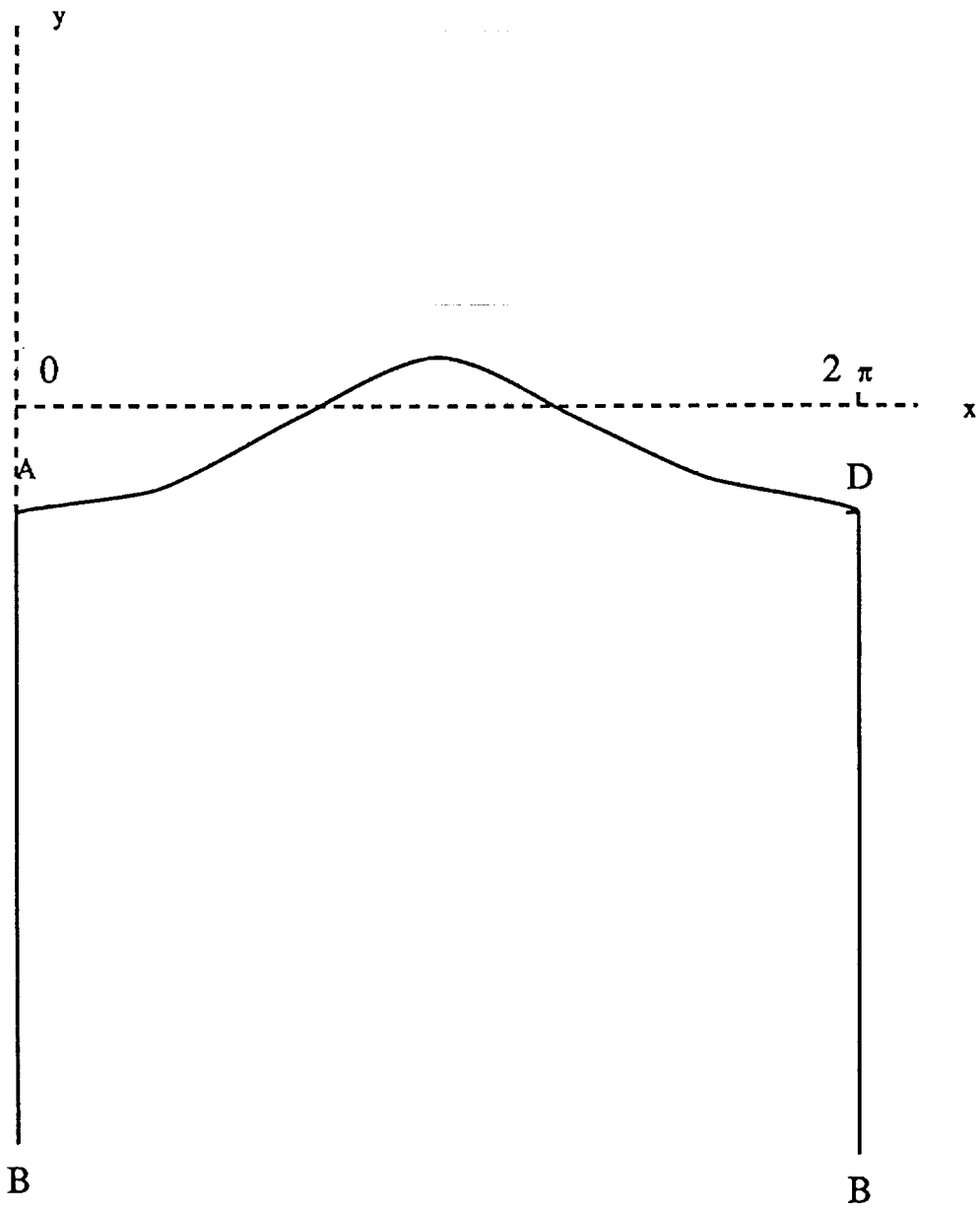

Fig. 2: The physical $z = x + iy$ plane.

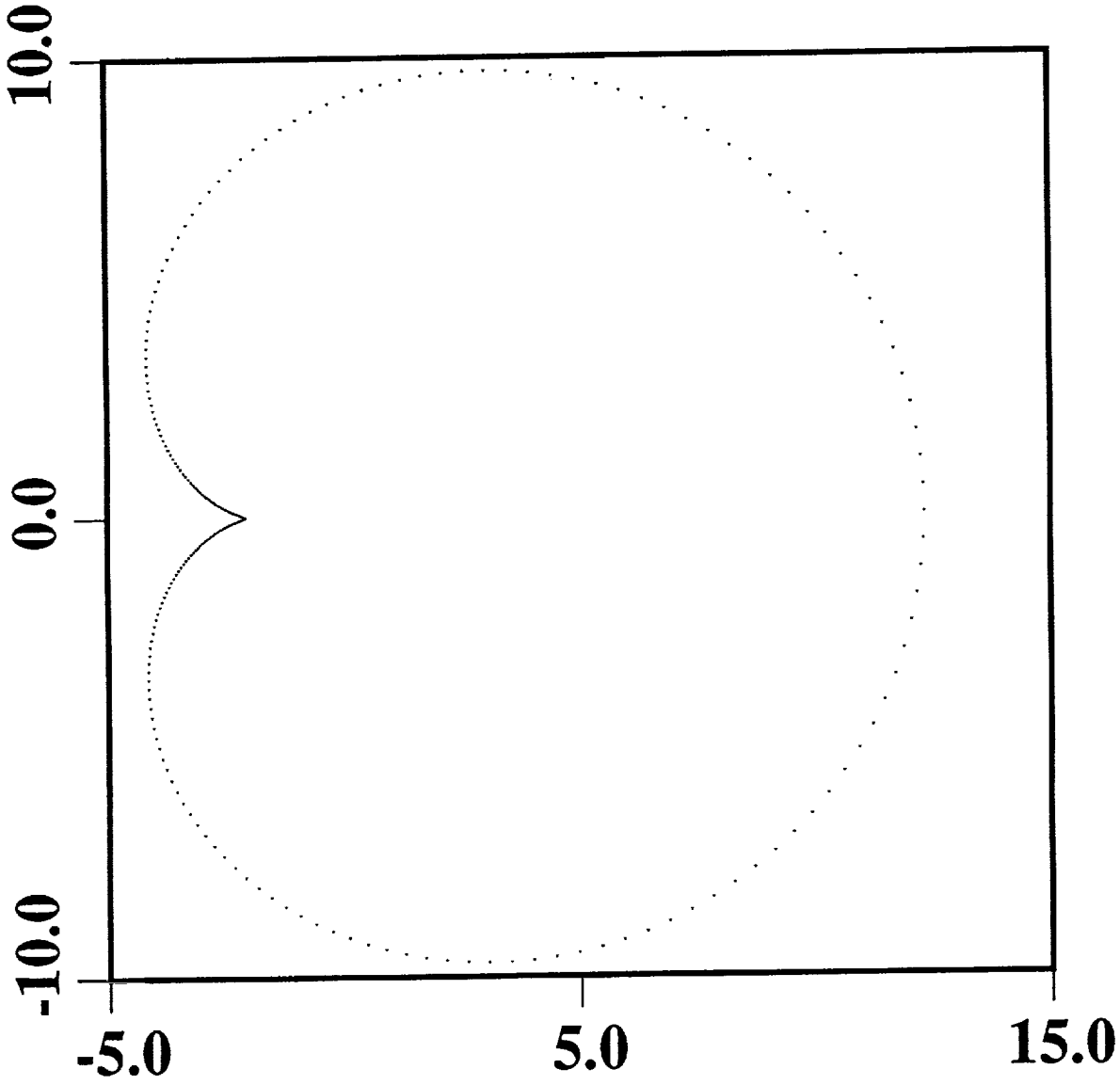

Fig. 3: The image of 256 uniformly spaced out points on $|\xi| = \rho_0 = 5$ at $t = 1.4$, just before the crossing of ξ_0 into $|\xi| < 5$.

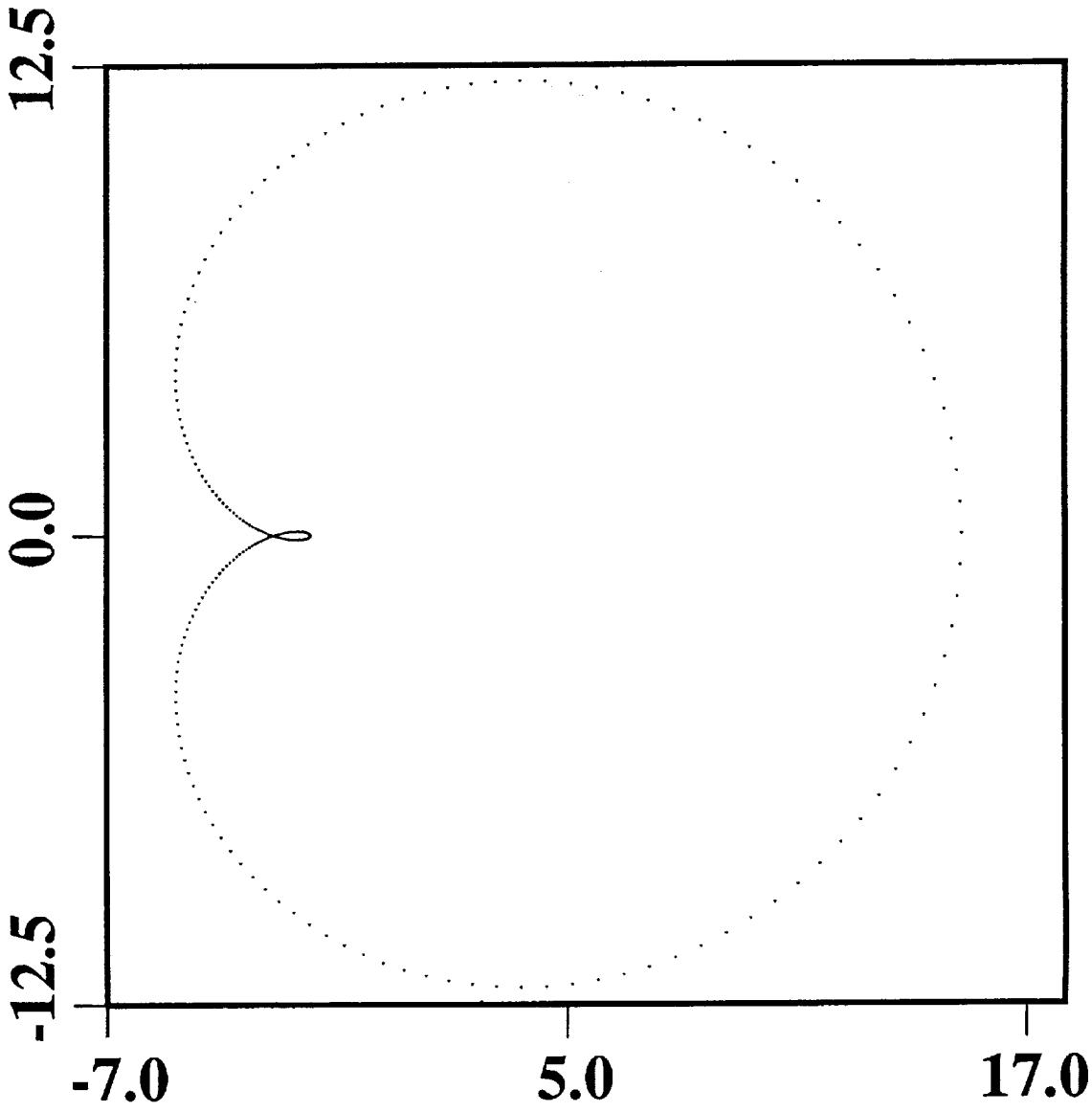

Fig. 4: The image of 256 uniformly spaced out points on $|\xi| = \rho_0 = 5$ at $t = 1.6$, a little after ξ_0 has crossed into $|\xi| < 5$.

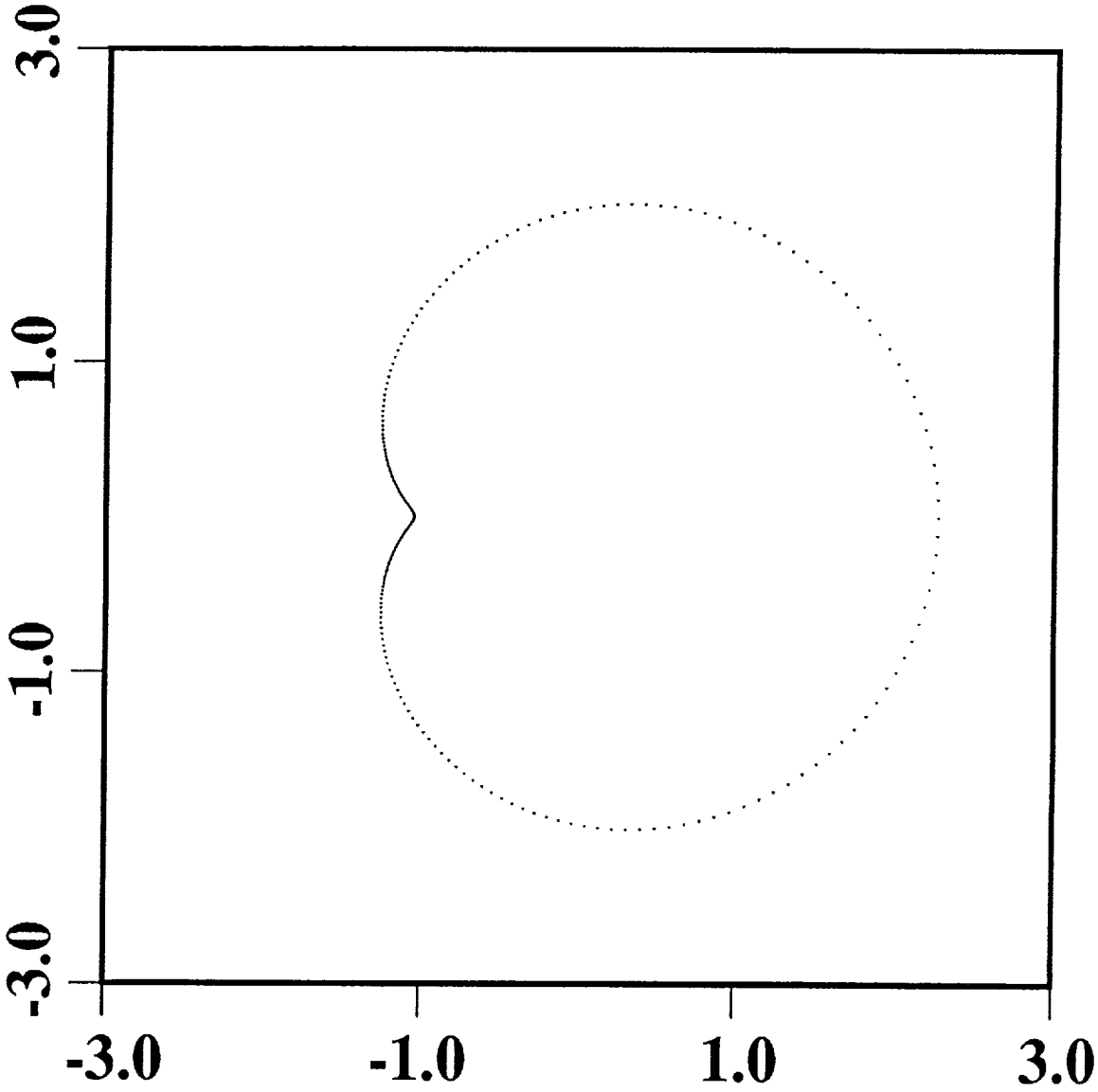

Fig. 5: The image of 256 uniformly spaced out points on $|\xi| = \rho_1 = 1.5$ in the ζ plane at $t = 2.4$, which remains a simple curve.

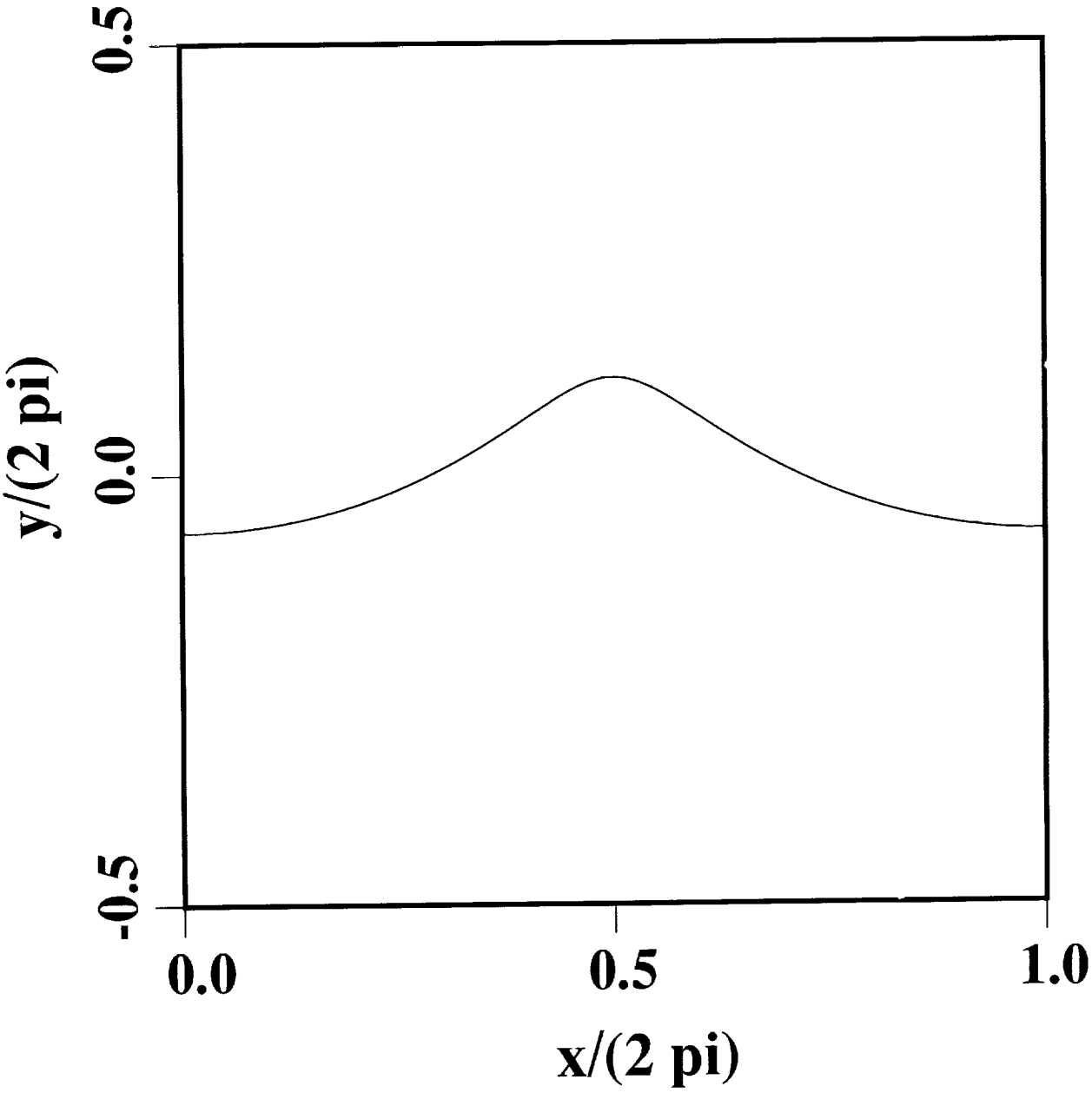

Fig. 6: The shape of the interface at $t = 2.4$ when normalized by the wavelength 2π. A spike can be noted at $\frac{x}{2\pi} = 0.5$ corresponding to $\zeta = -1$.

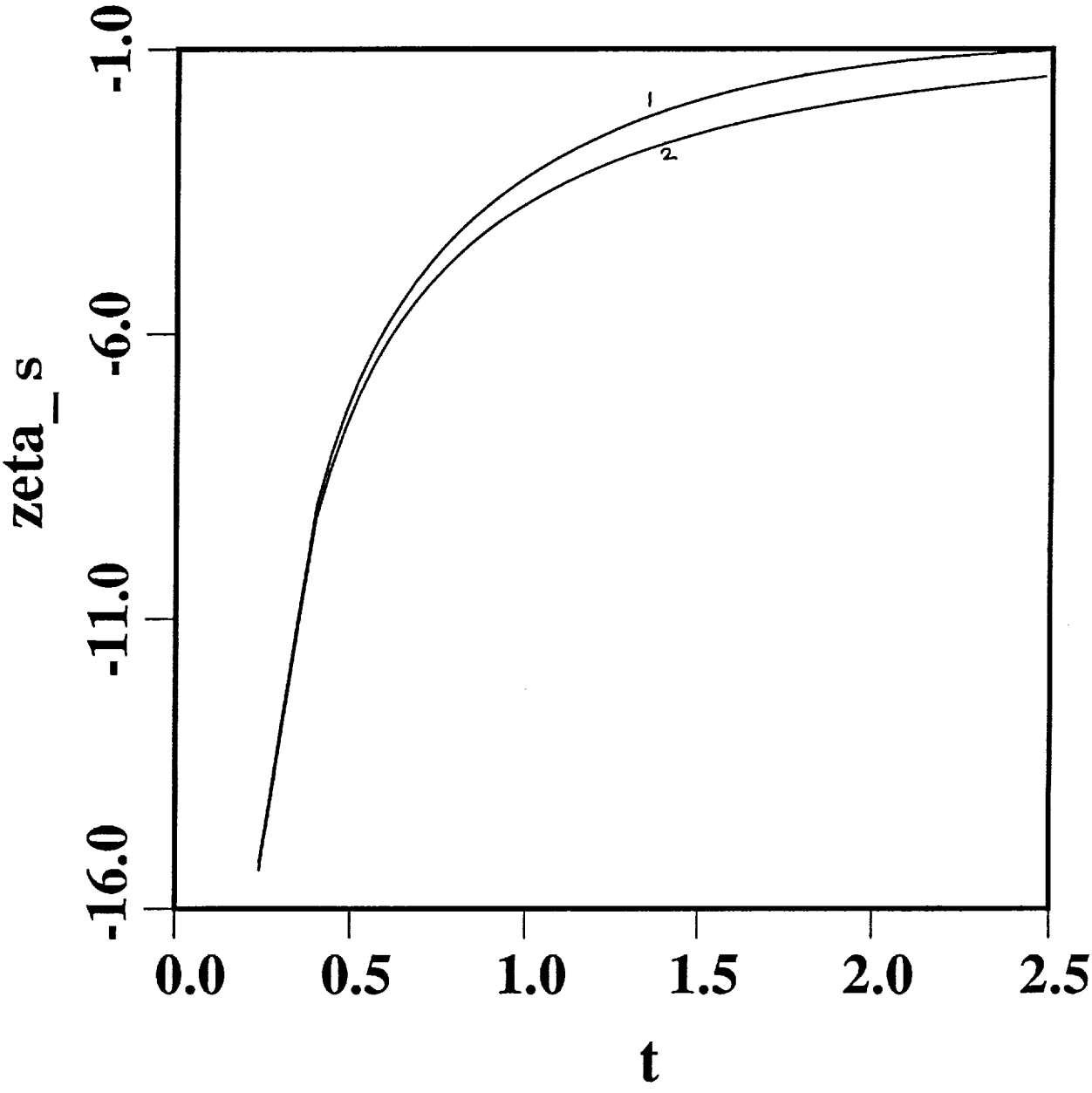

Fig. 7: The trajectory of the singularity $\zeta_s(t)$ as a function of t is shown by the curve marked 1. Curve 2 correspond to the analytical prediction (4.45) using a small t analysis.

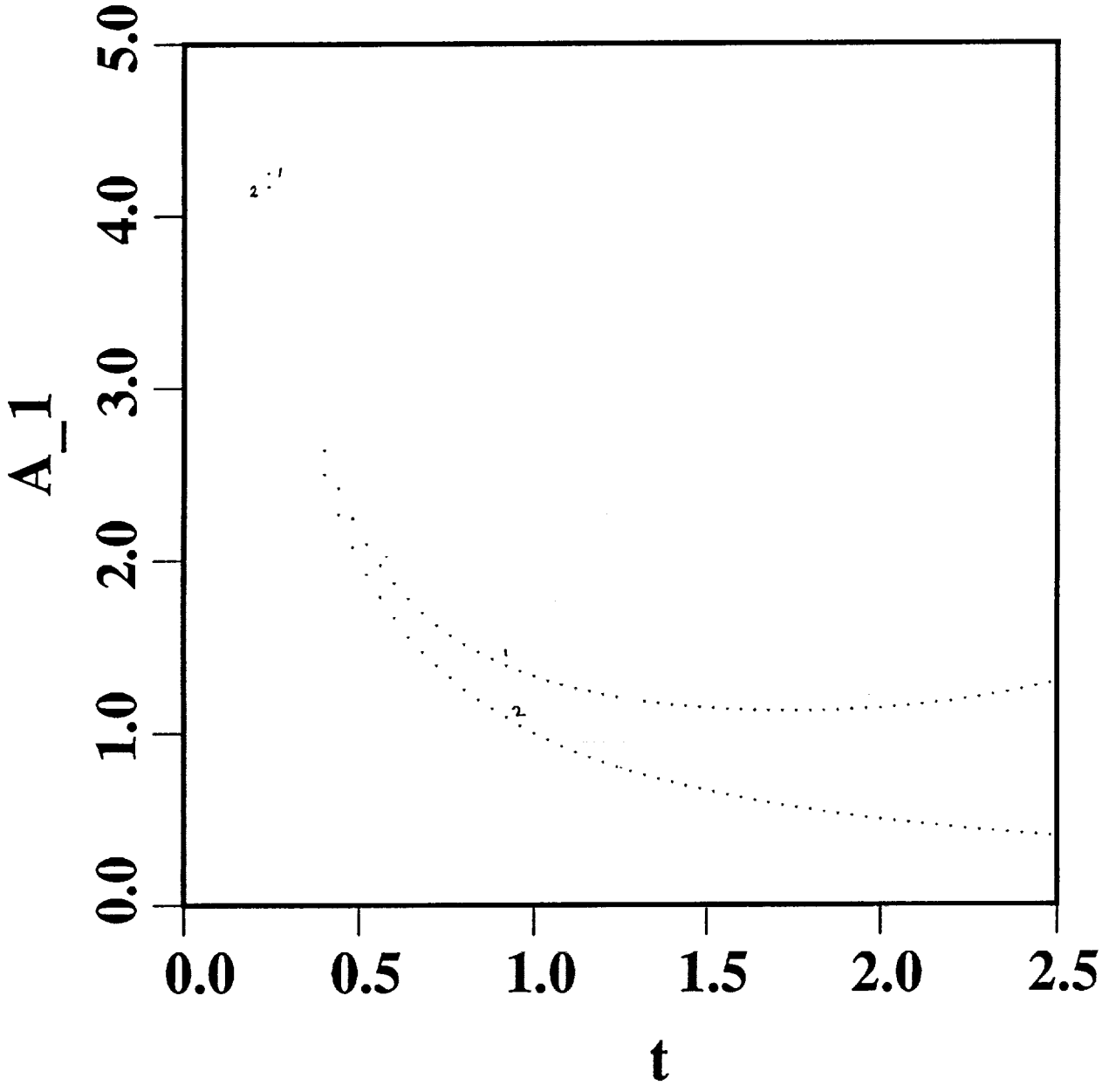

Fig. 8: A_1 is shown here as a function of t in the curve 1. Curve 2 corresponds to the analytical prediction using small t analysis.

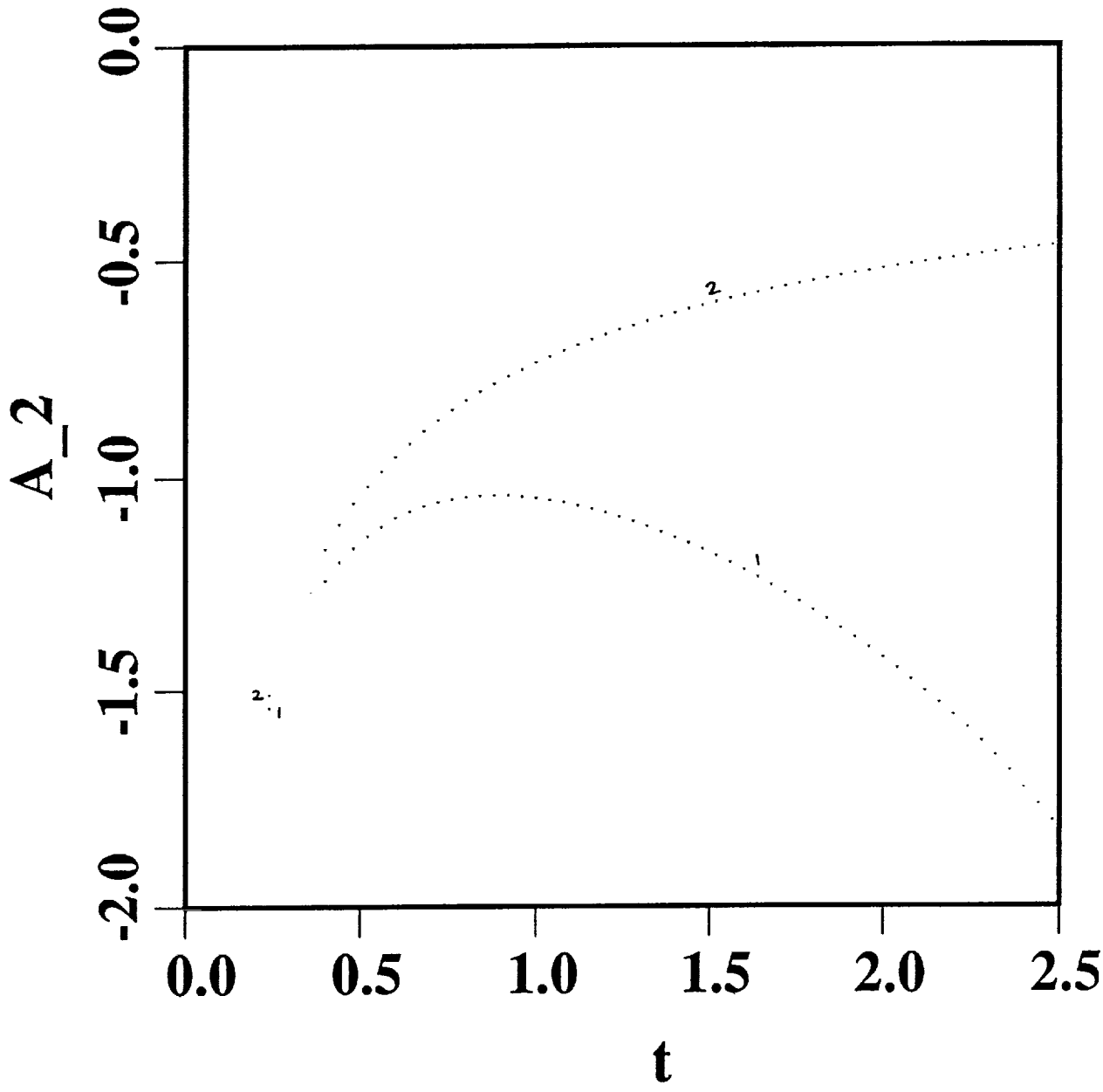

Fig. 9: A_2 is shown here as a function of t in the curve 1. Curve 2 corresponds to the analytical prediction using small t analysis.

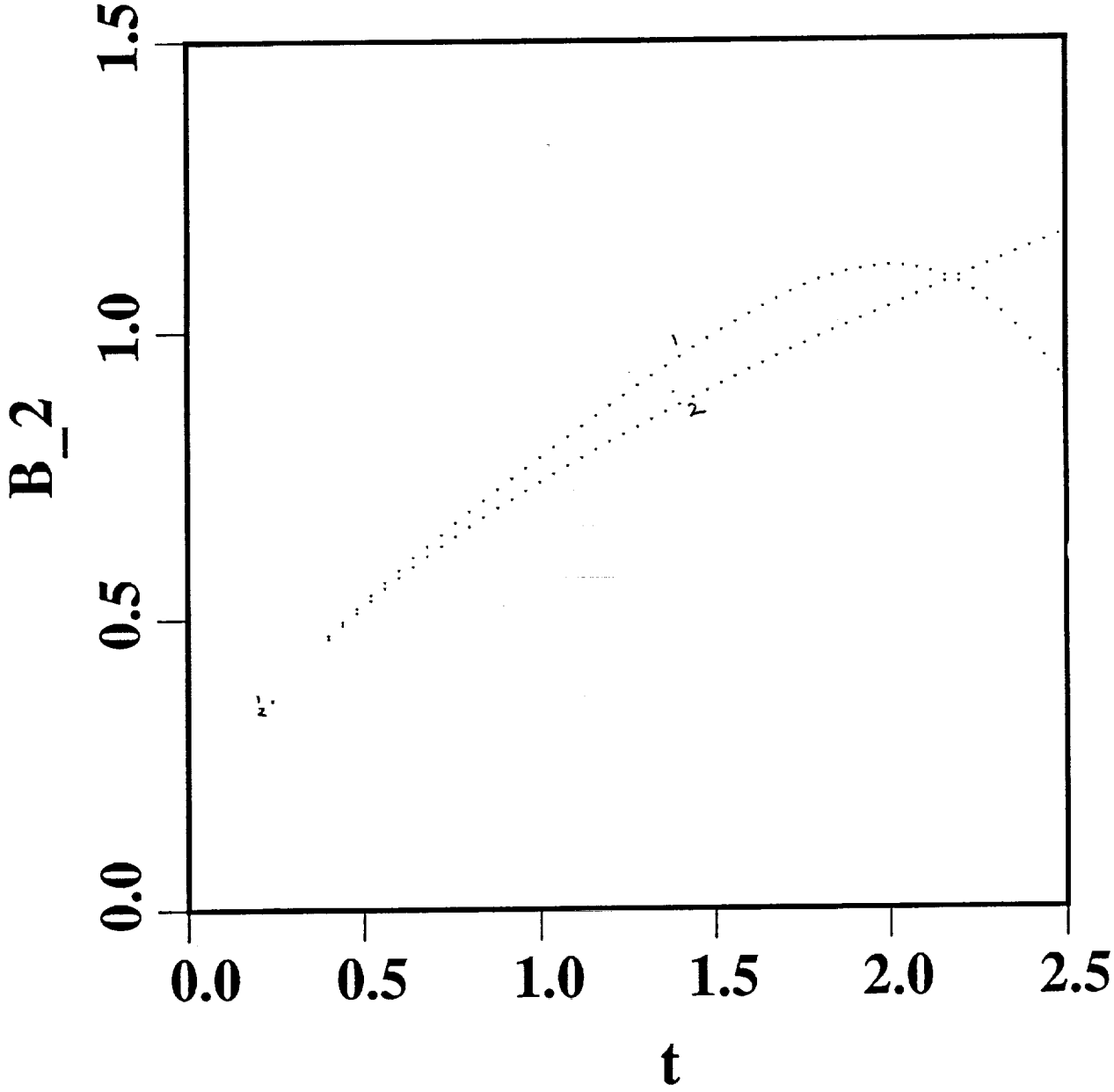

Fig. 10: B_2 is shown here as a function of t in the curve 1. Curve 2 corresponds to the analytical prediction using small t analysis.

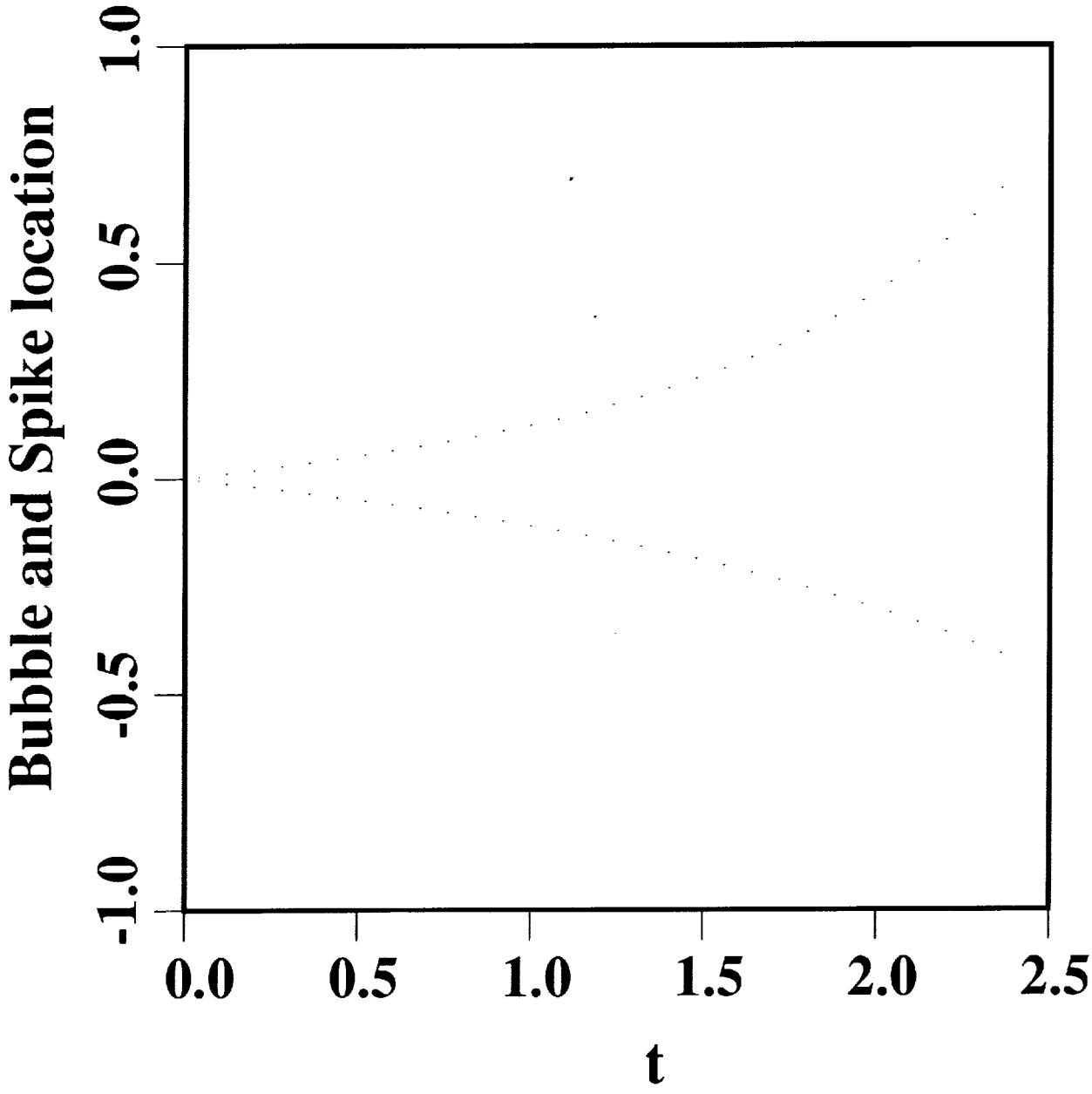

Fig. 11: Plot of $Im\ z(1,t)$ and $Im\ z(-1,t)$, the vertical location of the bubble-tip and the spike as a function of t.

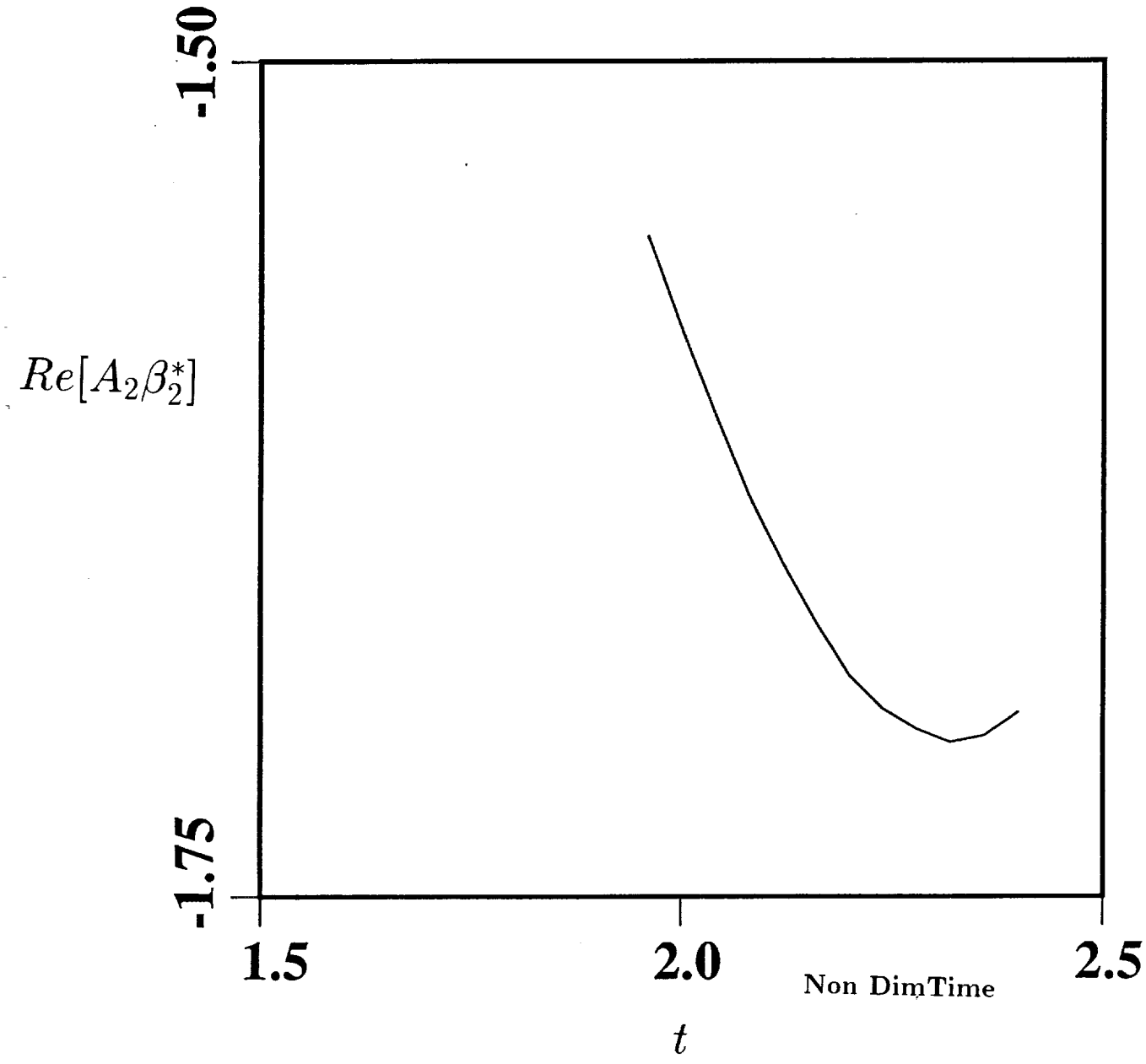

Fig. 12: Plot of $Re[A_2 B_2^*]$ against t.

REPORT DOCUMENTATION PAGE

Form Approved
OMB No. 0704-0188

1. AGENCY USE ONLY (Leave blank)	2. REPORT DATE	3. REPORT TYPE AND DATES COVERED
	August 1992	Contractor Report

4. TITLE AND SUBTITLE
SINGULARITIES IN THE CLASSICAL RAYLEIGH-TAYLOR FLOW: FORMATION AND SUBSEQUENT MOTION

5. FUNDING NUMBERS
C NAS1-18605
WU 505-90-52-01

6. AUTHOR(S)
S. Tanveer

7. PERFORMING ORGANIZATION NAME(S) AND ADDRESS(ES)
Institute for Computer Applications in Science and Engineering
Mail Stop 132C, NASA Langley Research Center
Hampton, VA 23665-5225

8. PERFORMING ORGANIZATION REPORT NUMBER
ICASE Report No. 92-37

9. SPONSORING/MONITORING AGENCY NAME(S) AND ADDRESS(ES)
National Aeronautics and Space Administration
Langley Research Center
Hampton, VA 23665-5225

10. SPONSORING/MONITORING AGENCY REPORT NUMBER
NASA CR-189690
ICASE Report No. 92-37

11. SUPPLEMENTARY NOTES
Langley Technical Monitor: Michael F. Card
Final Report
Submitted to Proc. Roy. Soc. London A

12a. DISTRIBUTION/AVAILABILITY STATEMENT
Unclassified - Unlimited

Subject Category 34, 59

12b. DISTRIBUTION CODE

13. ABSTRACT *(Maximum 200 words)*

This paper is concerned with the creation and subsequent motion of singularities of solution to classical Rayleigh-Taylor flow (two dimensional inviscid, incompressible fluid over a vacuum). For a specific set of initial conditions, we give analytical evidence to suggest the instantaneous formation of one or more singularity(ies) at specific point(s) in the unphysical plane, whose locations depend sensitively to small changes in initial conditions in the physical domain. One-half power singularities are created in accordance with an earlier conjecture; however, depending on initial conditions, other forms of singularities are also possible.

For a specific initial condition, we follow a numerical procedure in the unphysical plane to compute the motion of a one-half singularity. This computation confirms our previous conjecture that the approach of a one-half singularity towards the physical domain corresponds to the development of a spike at the physical interface. Under some assumptions that appear to be consistent with numerical calculations, we present analytical evidence to suggest that a singularity of the one-half type cannot impinge the physical domain in finite time.

14. SUBJECT TERMS	15. NUMBER OF PAGES
singularities; Rayleigh-Taylor flow	43
	16. PRICE CODE A03

17. SECURITY CLASSIFICATION OF REPORT	18. SECURITY CLASSIFICATION OF THIS PAGE	19. SECURITY CLASSIFICATION OF ABSTRACT	20. LIMITATION OF ABSTRACT
Unclassified	Unclassified		

NSN 7540-01-280-5500

Standard Form 298 (Rev. 2-89)
Prescribed by ANSI Std. Z39-18
298-102

NASA-Langley, 1992